

POLITECNICO DI TORINO

**Master degree course
in Biomedical Engineering**

Master thesis

Magnetoplasmonic nanoparticles for photothermal therapy



Supervisor

prof. Enrica Vernè
dott. Marta Miola

Student

Ormelli Cesare

April 2019

TABLE OF CONTENTS

SUMMARY	i
Preface.....	vi
1. Introduction	1
1.1 Nanomaterials	1
1.2 Type of nanoparticles	1
1.3 Nanomaterials applications: cancer therapy	3
2. Iron oxide Nanoparticles	7
2.1 Types of Iron Oxide Nanoparticles	8
2.2 Synthesis Approaches	9
2.3 Magnetic properties	15
2.3.1 Basics of Magnetism	15
2.3.2 Principles of magnetic heating	18
2.4 Colloidal properties	25
2.5 Biocompatibility	26
2.6 Surface coating	27
3. Iron Oxide – Ag/Au Nanocomposites	32
3.1 Structure and synthesis of Iron Oxide – Metal Nanocomposite	33
3.1.1 Synthesis of Ag nanoparticles	34
3.1.2 Synthesis of Au nanoparticles	35
3.2 Combined magneto-optical properties	36
3.2.1 Surface Plasmon Resonance	36
3.2.2 Mie Theory	37
3.3 Application of iron oxide-Ag/Au nanoparticles	38
3.3.1 Theranostic: Hyperthermia	38
4. Materials and methods.....	41
4.1 Materials	41
4.2 Methods	41
4.2.1 First route	42
4.2.2 Second route	46
4.3 Characterization techniques	47
5. Results and Discussions	52

5.1 Size and morphology	52
5.1.1 First synthesis route	52
5.1.2 Second synthesis route	57
5.2 Magnetic properties	62
5.3 Optical properties.....	64
5.3.1 Thermal experiments	66
5.4 Hemotoxicological properties	68
6. Conclusions and future developments.....	71
Acronyms	74
Symbols and constants	75
Acknowledgements	76
References	77

SUMMARY

1. Introduzione

Le nanotecnologie sono un campo di ricerca in rapida evoluzione che prevedono nuove possibilità applicative nel campo dei materiali, dell'elettronica, della litografia, della purificazione dell'acqua, dei sistemi energetici, della medicina e della farmacologia, delle produzioni alimentari e della nutrizione, dell'informatica e delle telecomunicazioni. La nanotecnologia si sta proiettando rapidamente anche sul mercato del settore medico (nano medicina), con nuove applicazioni nel campo dell'imaging, della somministrazione dei farmaci e trattamento dei tumori e con la realizzazione di protesi maggiormente resistenti e biocompatibili. La nano medicina ha l'obiettivo di rendere significativamente più efficace la diagnosi medica e la terapia. In campo terapeutico, le nanoparticelle possono essere usate ad esempio per realizzare sistemi alternativi di indirizzamento dei farmaci nell'organismo, come agenti di contrasto nella risonanza magnetica o come trattamenti ipertermici dei tumori.

2. Nanoparticelle di ossido di ferro (ION)

Le nanoparticelle magnetiche che vengono per lo più utilizzate per le applicazioni biomediche, sono di magnetite (Fe_3O_4), per la quale la suscettibilità è alta. Nanoparticelle magnetiche di ossido di ferro (Fe_3O_4 MNPs), note anche come SPIONs, presentano una elevate performance in termini di stabilità colloidale e biocompatibilità rispetto ad altre nanoparticelle metalliche. L'utilizzo di tali nanoparticelle magnetiche (MNPs) in applicazioni mediche è un settore che offre grandi potenzialità in campo terapeutico e nella diagnostica in vitro e in vivo. Le nanoparticelle possiedono proprietà magnetiche che offrono grandi vantaggi che possono essere utili, ad esempio, per consentire la manipolazione e il trasporto nella posizione desiderata attraverso il controllo di un campo magnetico prodotto da un elettromagnete o magnete permanente. Le loro proprietà magnetiche dipendono dalla dimensione, forma, struttura, cristallinità, metodo di sintesi e chimica di superficie della nanoparticella. La classificazione delle proprietà magnetiche di MNPs si basa sulla loro suscettibilità magnetica (χ), che è definita come il rapporto tra la magnetizzazione indotta ed il campo magnetico applicato.

Le tre principali applicazioni degli SPIONs in medicina sono: Imaging (le nanoparticelle, magnetizzandosi, aumentano notevolmente l'efficacia di alcune tecniche quali risonanza magnetica), drug delivery (tali particelle sono in grado di ancorare sulla superficie farmaci specifici e di formare un ferrofluido che può essere messo in movimento tramite l'utilizzo di campi magnetici esterni anche in grado di stimolare il rilascio del farmaco) e l'ipertermia, argomento di interesse e trattato in questa tesi. Ricordando che le cellule tumorali mostrano una minore resistenza agli aumenti di temperatura, le nanoparticelle vengono utilizzate come sorgenti di calore per aree molto ridotte; essendo anche in grado di controllare l'energia prodotta, le nanoparticelle risultano estremamente utili nell'applicazione di questa terapia.

Tuttavia, nonostante l'ampia gamma di applicazioni con buoni riscontri, tali nanoparticelle magnetiche sono caratterizzate da una forza tendenza a formare aggregati in soluzioni acquose: a causa di questo, di rilevante importanza è la loro funzionalizzazione superficiale. Tra i diversi possibili surfattanti adottabili, l'acido citrico si è dimostrato come la migliore soluzione, in grado di garantire un'ottima dispersione delle nanoparticelle: la de-protonazione dei gruppi terminali (-COOH) in ambiente fortemente basico dona alle nanoparticelle una carica superficiale fortemente negativa (-COO⁻), alla base dell'omogenea distribuzione in soluzione.

3. Nanocompositi ION – Ag/Au

L'obiettivo principale dell'ottenimento di tali nanocompositi è sfruttare le proprietà combinate di nanoparticelle di ossido di ferro e le nanoparticelle di questi due metalli nobili, in modo da essere in possesso di un raffinato strumento teranostico.

In questa tesi si vuole quindi sfruttare la combinazione tra la cosiddetta ipertermia foto-indotta, fenomeno che sfrutta la proprietà intrinseca delle nanoparticelle di metalli nobili Ag e Au detta SPR, che sono cioè in grado di restituire calore a seguito di irraggiamento, e l'ipertermia indotta magneticamente, proprietà intrinseca delle nanoparticelle di magnetite.

Per immobilizzare i metalli sulle ION, il (3-amminopropil) trietossisilano (APTES) risulta essere la soluzione migliore, grazie alla particolarità di esporre gruppi amminici terminale (-NH₂) che possono essere utilizzati per attaccare diverse biomolecole, farmaci o, appunto, metalli. La formazione di un sottile film di silano a seguito della funzionalizzazione con APTES, non solo non influisce sulle proprietà magnetiche del core di magnetite, ma garantisce anche un'ottima barriera contro agenti acidi o basici e ulteriore stabilità e dispersione alle nanoparticelle in soluzione.

Obiettivi della tesi

L'obiettivo principale di questo studio è l'ipotesi di utilizzare l'acido tannico come agente riducente durante la reazione di seeding dei sali metallici in nanoparticelle di oro e argento sulla superficie delle nanoparticelle di magnetite. Attraverso lo studio condotto all'Istituto Jozef Stefan presso Lubiana (SLO), diversi test sono stati effettuati per verificare l'applicabilità dell'ipotesi formulata. Una seconda ipotesi, infine, testata è la possibilità di usare tale acido tannico non solo come agente riducente, ma anche come stabilizzante, alleggerendo di molto la sintesi "canonica".

4. Materiali e metodi

Tutti i reagenti sono stati acquistati presso SIGMA-ALDRICH® e PANREAC®; le soluzioni acquose di nanocompositi magnetite e metallo nobile (Ag/Au) sono state sintetizzate presso il dipartimento di Scienze dei Materiali presso il Politecnico di Torino.

Una caratterizzazione chimico-fisica delle particelle è stata effettuata grazie all'impiego di:

- TEM (Transmission Electron Microscopy), STEM (Scanning Transmission Electron Microscopy) e DLS per un'analisi riguardante morfologia e dimensione dei nanocompositi;
- FT-IR (Fourier Transform Infrared spectroscopy), EDS (Energy Dispersive X-ray Spectroscopy) per un'analisi strutturale ed elementale;
- UV-vis (Ultraviolet-visible spectroscopy), VSM (Vibrating Sample Magnetometer), ICP-MS (Inductively Coupled Plasma mass spectrometry), laser per un'analisi mirata alle proprietà magnetiche, ottiche e termiche.

Infine, quindi, è stato possibile effettuare anche test ematotossicologici, grazie alla gentile concessione di cellule rosse di sangue ovino da parte della facoltà di Veterinaria dell'università di Lubiana (SLO).

Per quanto riguarda i metodi di sintesi delle nanoparticelle, si sono intraprese due strade:

1. *First synthesis route*: le nanoparticelle di magnetite, a seguito della co-precipitazione, sono state funzionalizzate tramite acido citrico e APTES. In seguito, sono stati uniti alle nanoparticelle di magnetite formate i sali dei metalli di Ag/Au e fatti precipitare tramite l'utilizzo di acido tannico, in questo caso contemplato solo come agente riducente.
2. *Second synthesis route*: le nanoparticelle, a seguito di co-precipitazione, sono state funzionalizzate utilizzando acido tannico, il quale poi viene ripreso anche per la precipitazione delle nanoparticelle di oro e argento. In questo caso, quindi, esso ricopre la funzione di stabilizzante e riducente.

5. Risultati

Nella sezione “Results and discussions” sono riportati tutti i grafici e le immagini risultanti dei test effettuati durante la parte sperimentale.

Diverse immagini risultano dall'analisi dimensionale e morfologica dei campioni e marcano le prime differenze tra i due diversi metodi di sintesi: risulta chiaro, infatti, come l'utilizzo del primo metodo di sintesi riesca a garantire la precipitazione di nanoparticelle di oro e argento di minori dimensioni rispetto al secondo, e, in generale, una migliore funzionalizzazione della magnetite con questi due metalli nobili.

I risultati provenienti dall'analisi con ICP-MS hanno permesso, poi, di determinare la concentrazione dei campioni e, quindi, di definire due concentrazioni fisse alle quali normalizzare tutti i campioni per le prove successive: c_1 (100 $\mu\text{g/ml}$) e c_2 (35 $\mu\text{g/ml}$).

Le figure 5.18 e 5.19 riportano i risultati dell'analisi ottica, i cui picchi di assorbimento possono poi essere ricondotti alle curve di riscaldamento delle figure 5.20 e 5.21: i test termici sono stati condotti per ogni campione irraggiandoli con un laser (potenza 1 W e lunghezza d'onda 808 nm) per 10 minuti.

Infine, nella tabella 5.4, sono raccolti i risultati dei test emotossicologici: in generale, tutti i campioni sono caratterizzati da una tossicità trascurabile per cellule sane.

6. Conclusioni

Nel capitolo finale si commentano i risultati ottenuti e si evidenziano le problematiche riscontrate: infatti, risulta che, a differenza di quanto sperato, l'acido tannico, seppur ottimo

agente riducente, non può essere comparato all'azione di acido citrico e APTES come agente stabilizzante; vengono pertanto, infine, suggerite ottimizzazioni volte ad abbattere queste limitazioni e poter usufruire dell'acido tannico sia come riducente ottimizzato sia come stabilizzante.

Preface

Following the urge to obtain new "smart" nanomaterials, the application of nanotechnology to medicine (nanomedicine) is developing towards new employments of great impact. This is the case of hyperthermia, where superparamagnetic and plasmonic nanoparticles are investigated as nanoheaters or nanotransducers, which can be activated remotely by radiations minimally harmful to physiological tissue and fluids. Furthermore, iron oxide - gold/silver nanocomposites offer the combination of the unique features of both gold/silver and iron oxide nanomaterials to enable applications in diagnostic and therapeutic environments.

In this work, a detailed study of the aqueous synthesis of iron oxide - gold/silver nanocomposites is presented. This method uses citric acid as stabilizing agent and (3-aminopropyl)triethoxysilane (APTES) for the dual functions of attaching fine gold and silver nanoparticles onto the magnetite surface as well as preventing the formation of aggregates. The reduction of the metal nanoparticles was achieved thanks to tannic acid. In addition, the possible further applicability of tannic acid as stabilizing agent is analyzed. Morphology, structure, composition and stability were characterized with Transmission electron microscopy (TEM), scanning transmission electron microscopy (STEM), energy-dispersive X-ray spectroscopy (EDS), Fourier transform infrared spectroscopy (FT-IR) and ζ potential. Magnetic and optical properties were analyzed with vibrating sample magnetometry (VSM) and ultraviolet – visible spectroscopy. These structures maintained the optical and magnetic features of gold/silver and iron oxide nanoparticles.

1. Introduction

1.1 Nanomaterials

Nanomaterials are devices of nanometric dimensions (1-100 nm). At this scale, some materials show interesting optical, electronic, catalytic, thermodynamic and electrochemical properties, which are influenced by their shape and chemical composition too.

Nanometric particles are in the same size range of some biomolecules, such as proteins, antibodies, membrane receptors and nucleic acids among others; this aspect, together with the high surface, volume ratio and the tunability of their properties, make these nanoparticles very powerful tools for imaging, diagnosis and therapy[1].

In the past few years nano-engineering and biomedical research gave birth to new technologies and new possible application in medicine. For many diseases, accurate diagnostic methods exist and are available but slow, expensive and requires a big amount of work to be executed. For other diseases, cancer for example, effective methods of diagnosis are still transitory.

It has been shown that, regarding biomedical applications, nanoparticles can be used at the same time for diagnosis and therapy, field called theranostic, granting high effectiveness to the treatments and, so, their specificity. Thank to this, the ability to target and treat only the cancerous cells and to diagnose any disease at its early stage is increased.[1]

1.2 Type of nanoparticles

Nanomaterials have the great ability to integrate with biological structures, this is at the base of nanomedicine in which the use of nanoparticles plays a fundamental role.

In particular, nanoparticles can be classified in two main categories: organic and inorganic ones.

-Organic nanoparticles: liposomes, dendrimers and carbon nanotubes.

- Liposomes: phospholipid vesicles (50-100 nm) composed of a bilayer membrane structure similar to that of biological membranes. Being amphiphilic, they can carry hydrophilic drugs within their aqueous interior as well as hydrophobic drugs dissolved into the membrane. Their surface can be modified with ligands or polymers to increase the delivery specificity.

- Dendrimers: synthetic polymers (<15 nm), constituted of a central core, an internal region a plenty terminal group that determine the dendrimer characteristic. They are excellent drug and imaging diagnosis agent carriers thanks to the modification of their multiple terminal groups.
- Carbon nanotubes: cylinders of coaxial graphite sheets (<100 nm), exhibit excellent strength and electrical properties and are efficient heat conductors. Used as biosensors, drug carriers and tissue-repairs scaffolds.

-Inorganic nanoparticles: such as quantum dots, magnetic, ceramics and metallic nanoparticles, have a central core that define their fluorescent, magnetic, electronic and optical properties.

- Quantum dots: colloidal fluorescent semiconductor nanocrystals (2-10 nm), photostable. Their central core consists of combination of elements from groups II-IV and III-V, coated with a layer of ZnS. Characterized by size and composition-tunable emission spectra and high quantum yield, as well as resistance to photobleaching, photo and chemical degradation, which make them excellent contrast agents for imaging and labels for bioassays.
- Metallic nanoparticles: They show localized surface plasmon resonance (absorbing light and emitting photons with the same frequency in all directions. Metallic nanoparticles are excellent labels for biosensors, being easily detectable with many techniques (optic absorption, fluorescence and electric conductivity).
- Magnetic nanoparticles: spherical nanocrystals (10-20 nm), with a Fe²⁺ and Fe³⁺ core often surrounded by a polymeric (e.g. dextran or PEG) shell. Excellent agents to label biomolecules and MRI contrast agents. Possible surface functionalization for active targeting.

Table 1.1 Examples of nanoparticles applications[1]

Nanoparticles component	Application	Indication
Liposomes	Drug delivery	Cancer
	Drug delivery	Vaccines: influenza, hepatitis A

	Drug delivery	Fungal infection
Dendrimers	Therapeutics	HIV, cancer, ophthalmology, inflammation
Carbon nanotubes	<i>In vitro</i> diagnostics	Respiratory function monitoring
	Imaging	Atomic-force microscopy probe tip
Quantum dots	<i>In vitro</i> diagnostics, imaging	Labelling reagents: Western blotting, flow cytometry, biodetection
Magnetic nanoparticles	<i>In vitro</i> diagnostic	Cancer
	Imaging, therapeutics	Liver tumors, cardiovascular disease, anemia
	Therapeutics	Cancer
Gold nanoparticles	<i>In vitro</i> diagnostics	HIV
	<i>In vitro</i> diagnostics, imaging	Labelling reagents (PCR, RNA, Western blotting), angiography and kidney

1.3 Nanomaterials applications: cancer therapy

Cancer is one of the leading death causes all over the world. The major problem nowadays is to be able to figure out the exact bound between the tumor biomarkers and the clinical pathology, as well as be able to detect and eliminate cancer without damaging other tissues at an early stage for maximum therapeutic benefit.[2]

Current therapy strategies are characterized by invasive processes, such as chemotherapy to minimize any cancer incidence, and surgery to delete as much neoplastic tissue as possible, followed by more chemotherapy and radiation: the high susceptibility to the action of these drugs and the high growth rate of the cancer can be used to delete its presence in healthy tissues.

Anyway, the efficacy of the treatment depends on its ability to target and destroy the cancer cell while affect as few healthy cells as possible; unfortunately, not all treatments are effective in killing the tumor, even if they are done with all the specifications needed, before it kills the patients.[2]

New cancer remedies are making their way developing in both terms of new agents against it and optimized delivering strategies, which leads to the nanomaterials.

The use of nanotechnology in cancer therapy puts forth the chance of destroying tumors while minimizing damage to other tissues and organs.

To deliver therapeutic agents to the tumor cells, few problems must be vanquished:

1. Physiological barriers, responsible of drug resistance at tumor level (non-cellular based mechanisms);
2. Drug resistance at cellular level;
3. Distribution, biotransformation and clearance of anticancer drugs in the body.

The occurrence of a clinical relapse after an initial positive response to the treatment or the lack of tumor size reduction can be entitled as clinical drug resistance. Inadequate vascularization of the cancer mass ca be responsible for this problem: hence, the access of the drugs is reduced, and the cancer cells are protected. Moreover, the acidic environment can prevent diffusion of these compounds across the cellular membrane, causing their ionization; diffusion that can be blocked also by high interstitial pressure and low microvascular pressure.[3]

As said, also cellular mechanisms can enhance tumor resistance to therapeutic intervention (altered activity of enzymes, altered apoptosis regulation or transport based), as well as transport based mechanisms, and are responsible for the multi-drug resistance (MDR), or multi-drug resistance associated protein (MRP). In the end, given that anti-tumor drugs are toxic also to healthy cells, their efficacy is deeply reduced.

A solution to this lack of selectivity can be reached by the association of antitumor drugs with colloidal nanoparticles: if planned properly, they can overcome all these problems and release the active agent in a specific place and time. This behavior can be reached taking advantage of two targeting strategies: active and passive.[2]

Nanocarriers can accumulate in the cancer interstitium because of the compromised lymphatics clearance in neoplastic tissues, principle called ‘enhanced permeability and retention effect’ (EPR); this, together with the feature of the surface for the nanocarriers, which is designed for

long permanence in the blood stream, is called 'passive targeting'. Furthermore, their surface can be functionalized with targeting ligands, which bind to specific receptors on the tumor cells and endothelium: this so called 'active targeting' enhance the selectivity of the delivery of drugs.

An advantage of these nanovectors -nanoparticles capable of transporting and delivering several bioactive molecules, including therapeutic agents and imaging contrast enhancers- is their ability to overcome various biological barriers and to localize into the targeted tissue.

The nanovectors that are used nowadays can be identified in the following groups or 'generations':

- i. First generations: localized in the tumor thanks to the EPR mechanism or to the enhanced permeability of the neoplastic tissue neovasculature, comprehend a container and an active principle; they're functionalized with a thin layer (e.g. PEG), which prevents their seizure by phagocytic blood cells, delaying the circulation time.
- ii. Second generation: characterized by the ability to respond to the environment and activate, also through antibodies or other biomolecules.
- iii. Third generation: characterized by more complex functions, such as time-controlled deployment of active nanoparticles across different biological barriers.

Another targeting method is the usage of gold nanoparticles, which are able to release heat when irradiated with a laser light, destroying selectively the tumor cell as a consequence of their high heat sensitivity.

Superparamagnetic nanoparticles, such as magnetite (Fe_3O_4), can be used as contrast agents to improve magnetic resonance imaging (MRI). The particle can be coated with a peptide that can bind with the tumor cell: at this stage, the magnetic properties of the iron oxide can be used to enhance the efficacy of the MRI, making it a powerful tool for discrimination between neoplastic and normal tissue. It is interesting, finally, how they can be conducted directly to the tumor or the area of interest for the treatment by an external magnetic field, taking advantage of their superparamagnetic feature. [2][3]

Research activity in improving cancer therapy has expanded tremendously in the last years, with new strategies of directing drugs and nanovectors to tumors as well as new types of drugs.

However, there is still a lot that can be done to treat and perhaps prevent cancer by handling it in as an early stage as possible.

2.Iron oxide Nanoparticles

In the last few years, nanotechnology has developed so much that nowadays it is possible to manufacture, characterize and specially to adapt the functional properties of the nanoparticles for biomedical and diagnostic applications.[4]

Among all, the investigation of iron oxide nanoparticles (IONs) has intensively increased in particular for their biomedical applications:

- Targeted drug delivery;
- Magnetic resonance imaging (MRI);
- Magnetic hyperthermia and thermoablation;
- Tissue repair;
- Biosensing;
- Cellular therapy[5]

For these applications, the particles must have combined properties of high magnetic saturation, biocompatibility and interactive function at the surface (these can be modified creating few atomic layers of organic polymer, inorganic metallic or oxide surfaces, that can be additionally functionalized attaching active biomolecules).

Their effectiveness depends on:

- i. High magnetic susceptibility for an effective magnetic enrichment;
- ii. Size of the particles should be in the range of 6-15 nm (in this range they are rapidly removed through extravasations and renal clearance);
- iii. Superparamagnetic behavior;
- iv. Tailored surface chemistry for specific biomedical applications; etc.

Above all, the superparamagnetic activity is of most interest; such characteristic grants them the feature to not retain any magnetism after removal of the magnetic field.[4]

They are classified as SPION (Superparamagnetic Iron Oxide Nanoparticles) or USPIO (Ultrasmall Superparamagnetic iron Oxide Nanoparticles) depending on their diameter (below 30 nm they are addressed as USPIO).

In this chapter types, synthesis methods and the properties of interest for biomedical application of the iron oxide nanoparticles are briefly reported.

2.1 Types of Iron Oxide Nanoparticles

Characterized by iron and oxygen, there are eight known different iron oxides; among these, three are most valuable: hematite ($\alpha\text{-Fe}_2\text{O}_3$), maghemite ($\gamma\text{-Fe}_2\text{O}_3$) and magnetite (Fe_3O_4). [5]

Hematite is the most stable iron oxide and semiconductor under ambient conditions. Widely used in catalysis, pigments and gas sensors thanks to its low cost and high resistance to corrosion, it can be used for the synthesis of the other two.

Magnetite is a ferrimagnetic material at room temperature containing both Iron(II) and Iron(III). Particles with a size less than 15 nm are superparamagnetic, although this is dependent also on the synthesis method. Proven to be biocompatible, with proper surface functionalization they can form ferrofluids (homogenous suspension in suitable solvents), that can interact with an external magnetic field and be positioned in a focused area, facilitating medical diagnosis (MRI) and AC magnetic field assisted cancer therapy.

Maghemite, finally, can be considered as a fully oxidized magnetite. It is superparamagnetic at room temperature. [5]

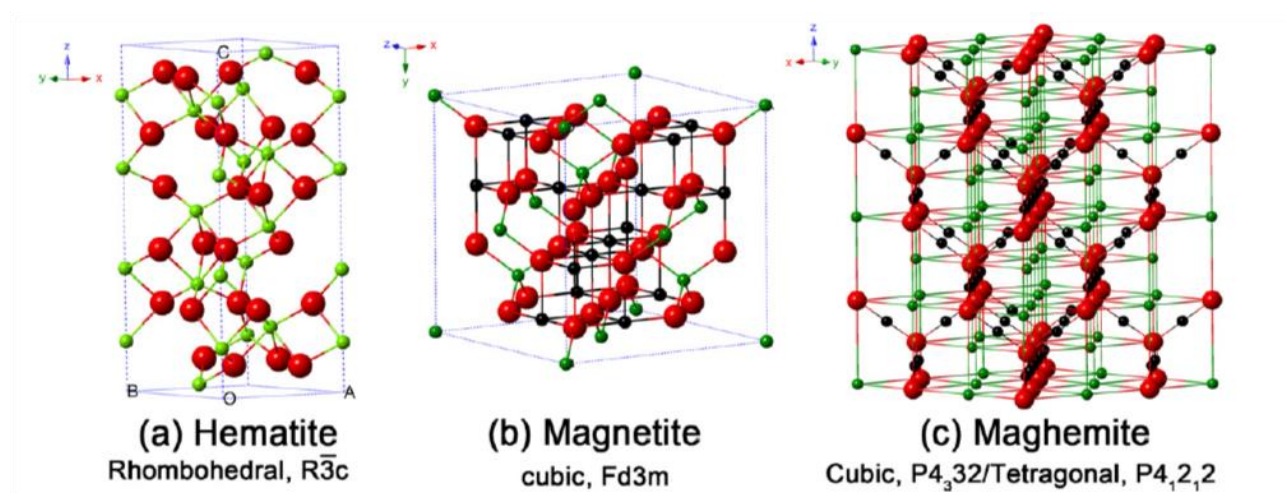


FIGURE 2.1. CRYSTAL STRUCTURE AND CRYSTALLOGRAPHIC DATA OF THE HEMATITE, MAGNETITE AND MAGHEMITE (THE BLACK BALL IS Fe^{2+} , THE GREEN BALL IS Fe^{3+} AND THE RED BALL IS O^{2-}). [5]

2.2 Synthesis Approaches

In the past decades, a lot has been done to find a facile and flexible synthetic route able to produce magnetic nanoparticles with the desired size and acceptable size distribution without aggregation.

According to the state of art, the most practiced synthesis routes can be grouped in:

- I. **Wet chemical synthesis:** co-precipitation, microemulsion, thermal decomposition, sol-gel processing, polyols, hydrothermal/solvothermal routes, sonochemical synthesis, micro-wave assisted synthesis;
- II. **Vapor/aerosol synthesis:** spray pyrolysis, laser pyrolysis.

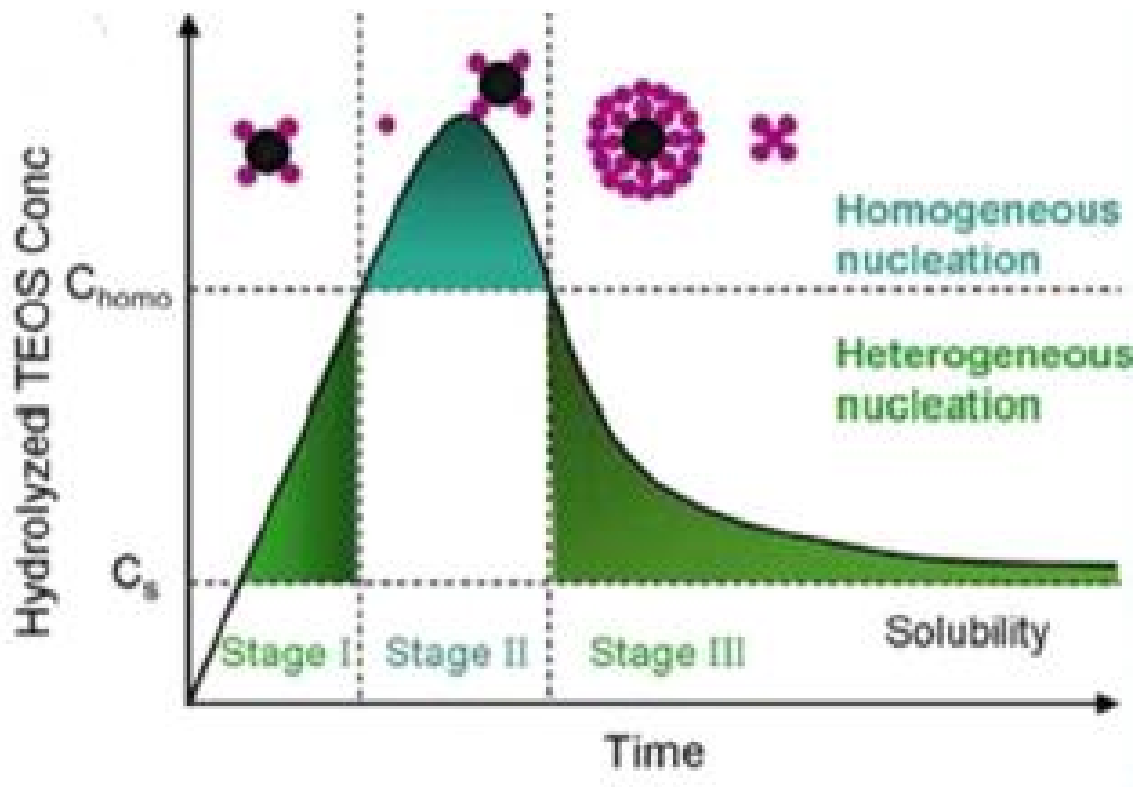


FIGURE 2.2 LAMER DIAGRAM: MECHANISM OF FORMATION OF UNIFORM PARTICLES IN SOLUTION[5]

Co-precipitation

It's the most conventional method and consists of mixing ferric and ferrous ions in a 1:2 molar ratio in very basic solution at room temperature; the size, shape and composition of the IONs

are directly subject to the experimental parameters, such as the types of iron salts (chlorides, perchlorates, sulfates etc.), Fe(II)/Fe(III) ratio, pH value and ionic strength of the medium.[6]

The overall reaction can be explained as follows:



In this case, a complete precipitation of Fe_3O_4 should be expected between pH 9 and 14. Furthermore, to inhibit their agglomeration, the nanoparticles so produced are usually coated with organic or inorganic molecules.[4]

There is another method for the synthesis in solution: ferrous hydroxide suspension is partially oxidized with different oxidizing agents, which guarantee that spherical magnetite particles can be obtained with a mean diameter between 30 and 100 nm from Fe(II) salt, a base and a mild oxidant.

Nevertheless, the first method is the most used for preparation of IONs useful in biotechnology application, thanks to its higher control on the mean size of the particles and to the possibility to obtain spherical particles homogeneous in size. [6]

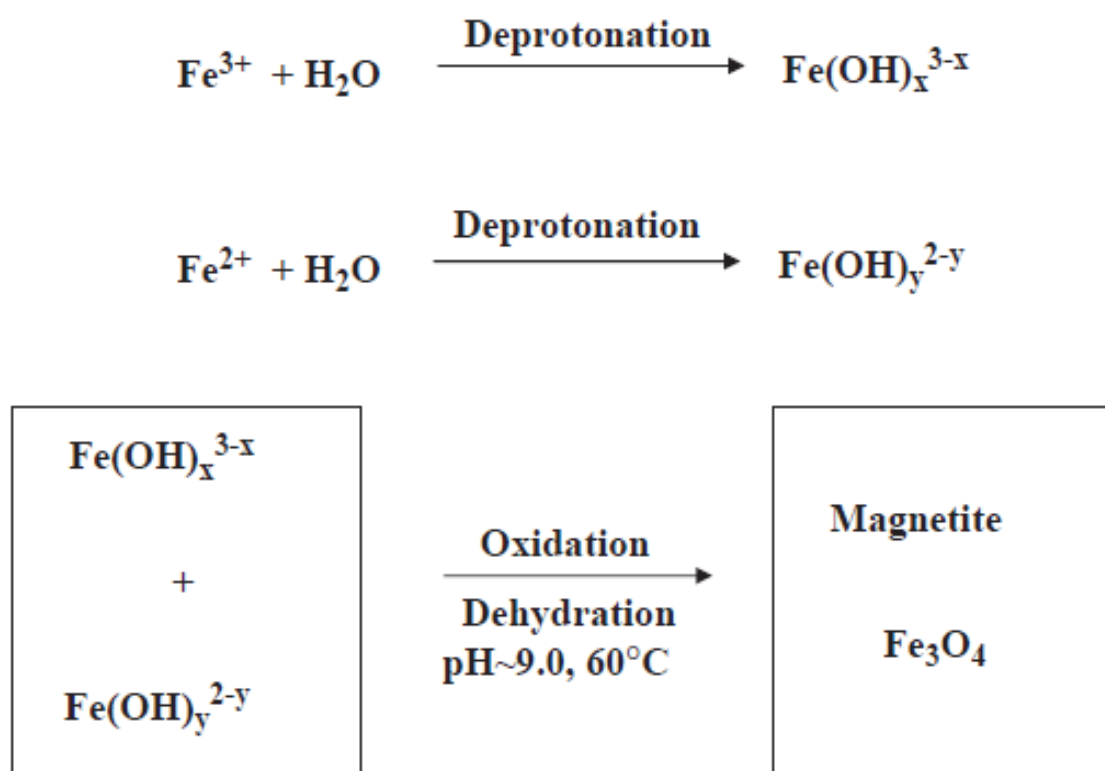


FIGURE 2.3 SCHEME SHOWING THE REACTION MECHANISM OF MAGNETITE PARTICLE FORMATION FROM AN AQUEOUS MIXTURE OF FERROUS AND FERRIC CHLORIDE BY ADDITION OF A BASE. THE PRECIPITATED MAGNETITE IS BLACK IN COLOR.[4]

Microemulsion

Isotropic liquid mixtures of oil, water and a surfactant (usually with additional co-surfactant). The two basic types of microemulsion are direct (water-in-oil, W/O) and reverse (oil-in-water, O/W), with the first being the most used to produce nanoparticles. [5], [6]

During the reaction, the surfactant can form a monolayer at the interface between oil and water, with the hydrophobic tails of its molecules dispersed in the oil phase whereas the hydrophilic heads in the water phase. This dispersed phase contains the metal salts or other ingredients and serves as a nano/micro-reactor, giving a confined environment for the nucleation and controlled growth of nanocomposites. The main advantage of utilizing microemulsion methodology to prepare SPIONs is that their size can be controlled by tuning the size of the micelles, formed by the surfactant.

Although this, difficulties related to hostile effects of residual surfactant on the properties of iron oxide particles and the impossibility to reach high temperatures (which means SPION with low crystallinity and in low yield) represent the biggest limits to this method.[7]

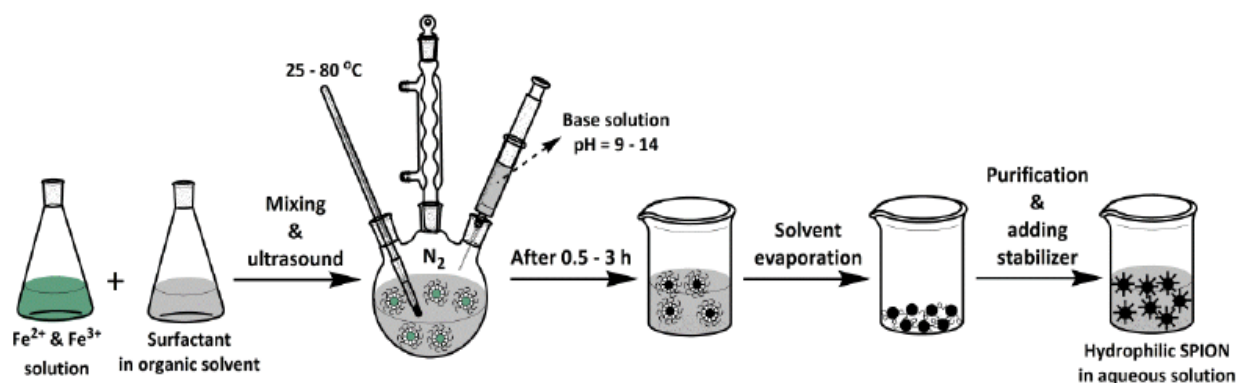


FIGURE 2.4 COPRECIPITATION OF SPION NANOPARTICLES VIA A W/O MICROEMULSION SYSTEM[7]

Thermal decomposition

One of the best methods to obtain high control over shape and size of the SPION, narrow size distribution and good crystallinity is the thermal decomposition of organometallic or iron precursors in organic solvents. This procedure displays superior properties (high quality in term of size, dispersion and crystallinity thanks to high temperature and surfactant) to those obtained with co-precipitation and microemulsion, since nucleation can be separated from the growth phase and complex hydrolysis reactions can be avoided. On the other hand, however, the use

of toxic chemicals, such as chloroform or hexane, makes this approach not environmentally friendly; moreover, because of the hydrophobic coating, an additional step is needed to make water-dispersible and biocompatible nanoparticles, which are only dissolved in non-polar solvents.[5],[7],[8]

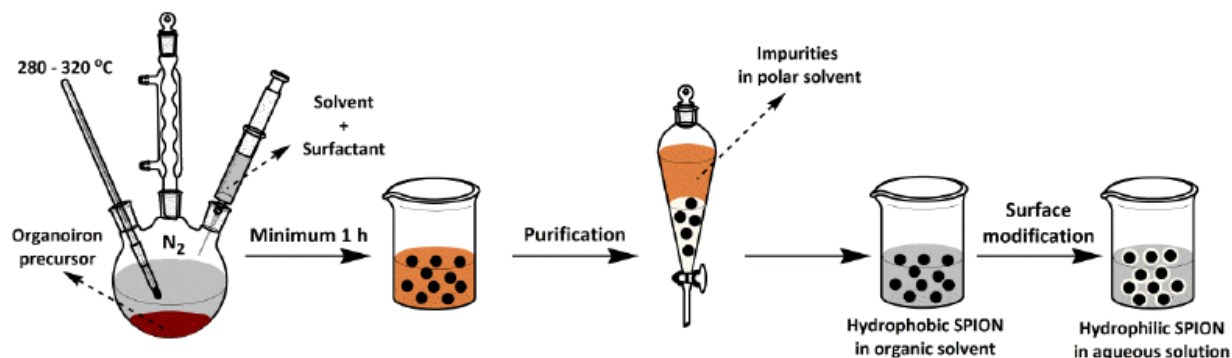


FIGURE 2.5 ILLUSTRATION OF THE THERMAL DECOMPOSITION PROCESS [7]

Sol-gel process

The process is based on the formation of colloidal sols thanks to the hydrolysis, condensation and gelation of a molecular precursor in an ethanol-aqueous solution, to obtain a 3D metal oxide network (wet gel); then, to get the ION, this gel requires another step after drying and gel removal.

However, adding surfactant before the gelation leads to the formation of nano-sized iron oxides without the 3D network.

This process provides a simple method to synthesize monodispersed and large-sized nanoparticles at ambient conditions. Still, due to the room conditions, heating treatments are needed to reach the desired crystallinity and, in addition, post-treatment for purification are required because of product contaminations. [5],[7]

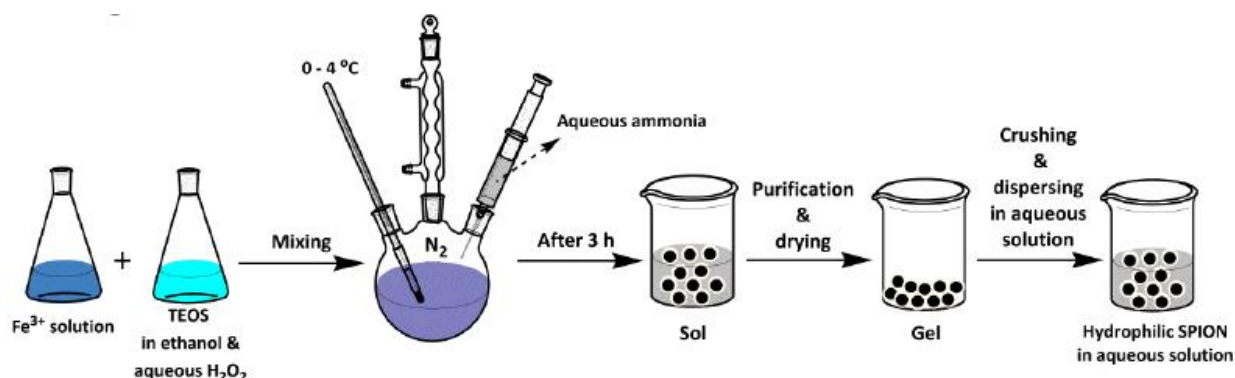


FIGURE 2.6 SCHEMATIC ILLUSTRATION OF THE SOL-GEL PROCESS[7]

Polyols

Metallic nanoparticles can be synthesized by the reduction of dissolved salts and direct metallic precipitation from a polyol containing solution. An iron precursor is suspended in a liquid polyol and then is stirred and heated to the boiling temperature of the solvent.

Well adapted for the preparation of IONs with different sizes and shapes, in this process the polyol can serve as solvent but also as reducing agent, which impede particle aggregation and control their growth. Along with the sol-gel process, a lot of advantages are granted by the polyol method (easy dispersed IONs in water, high crystallinity, high saturation magnetization), as well disadvantages, such as high cost of metal precursors and the need of safety consideration during the process.[5]

Hydrothermal routes

Called also solvothermal, when organic solvent is used in a non-aqueous system, the hydrothermal process is particularly appropriate for the growth of iron oxide nanocrystals with a maintenance of a good grade of control over their composition. Mostly used for the creation of IONs, the process involves the oxidation and mineralization of iron ions and, therefore, the crystallization of the substance in a sealed container from the high temperature aqueous or non-aqueous solution under high vapor pressure.

The process is very adaptable, it grants the possibility to create crystalline phases unstable at the melting point and to grow materials that a high vapor pressure near their melting point; on the other hand, however, despite being so versatile, it's characterized by a slow reaction kinetics at any given temperature. [5],[6],[7]

Sonochemical synthesis

Another interesting alternative to the methods mentioned before is the so called sonolysis (sonochemical or ultrasound irradiation): this procedure uses the effects of ultrasound (US) deriving from acoustic cavitation. Briefly, it consists of creation, growth and implosive collapse of bubbles in liquid: this localized implosion creates high temperature and high pressure, which are perfect conditions for the preparation of bare or functionalized IONs from aqueous ferrous salts. Despite it allows to have biocompatible nanoparticles with excellent colloidal properties

and uniformity of mixing and reduction of crystal growth (it leads to faster rates of reaction and chemical dynamics), the sonolysis method is not useful to realize the fabrication of IONs with controllable shapes and dispersion.[5],[7]

Microwave-assisted synthesis

Relatively recent process. Widely use for the creation of IONs with controllable size and shape. In particular, the microwave radiation results in strong agitation of the molecules; this translates in strong agitation, provided be their reorientation, in phase with the electrical excitation field which causes an intense internal heating. Hence, microwave-assisted process can decrease the processing time and energy cost, thanks to the instantaneous ‘in core’ heating of materials in a homogenous and selective manner, different from the classical ones. Due to the stabilization of the ION prepared with this method, they can be easily dispersed in water without other purification step. Such characteristic can be considered as attractive for fabrication of large-scale IONs.[5]

Spray pyrolysis

Easy, direct and continuous process to produce magnetic nanoparticles. The solid nanoparticle is obtained after the evaporation of the droplet of the solution and the condensation within it, followed by drying and thermolyzing of the precipitated particle at high temperature. Useful method to prepare colloidal aggregates of superparamagnetic nanoparticles. [6]

Laser pyrolysis

This procedure accentuates three particular characteristics: small particle size, narrow size distribution and the nearly absence of aggregation. It consists in a continuous carbon dioxide laser which heats a flowing mixture of gases; above a certain pressure and laser power, in the reaction zone amass a critical number of nuclei, which leads to a homogeneous nucleation of particles.

These particles so obtained are then filtered under the action of an inert gas.[6]

TABLE 2.1 SUMMARY COMPARISON OF THE SYNTHETIC METHODS FOR PRODUCING MAGNETIC IONS.[5]

Method	Reaction and conditions	Reaction temp. [°C]	Reaction period	Size distribution	Shape control	Yield
Co-precipitation	Very simple, ambient	20–150	Minutes	Relatively narrow	Not good	High/scalable
Thermal decomposition	Complicated, inert atmosphere	100–350	Hours-days	Very narrow	Very good	High/scalable
Hydro- or solvothermal synthesis	Simple, high pressure	150–220	Hours-days	Very narrow	Very good	High/scalable
Sol-gel and polyol method	Complicated, ambient	25–200	Hours	Narrow	Good	Medium
Microemulsion	Complicated, ambient	20–80	Hours	Narrow	Good	Low
Sonolysis or sonochemical method	Very simple, ambient	20–50	Minutes	Narrow	Bad	Medium
Microwave-assisted synthesis	Very simple, ambient	100–200	Minutes	Medium	Good	Medium
Biosynthesis	Complicated, ambient	Room temp.	Hours-days	Broad	Bad	Low
Electrochemical methods	Complicated, ambient	Room temp.	Hours-days	Medium	Medium	Medium
Aerosol/vapor methods	Complicated, inert atmosphere	>100	Minutes-hours	Relatively narrow	Medium	High/scalable

2.3 Magnetic properties

2.3.1 Basics of Magnetism

A lot of materials respond to the application of a magnetic field with their own magnetization, M , and so with their own magnetic field; that response, however, is usually weak and cannot exist without the original field.

When a substance is placed in a magnetic field, H (measured in Tesla), the intensity of its magnetization M is related to the field and to the magnetic susceptibility, k , which is an intrinsic feature of the material, and can be formulated in terms of volume as k , or in terms of mass as χ :

$$M = k H \quad (1)$$

The magnetic induction is described by the equation:

$$B = \mu_0 (H + M) \quad (2)$$

μ_0 is the vacuum permeability and M is the magnetic moment per volume. Magnetic permeability of the material μ is related to μ_0 and express the tendency of the magnetic field threads to pass through the same material; it's defined as:

$$\mu = \mu_0 (1 + k_B) \quad (3)$$

where k_B is the Boltzmann constant.

Magnetic permeability is the parameter that distinguishes paramagnetism ($\mu > 1$) from diamagnetism ($\mu < 1$).

Five different types of magnetism can be defined: paramagnetism, diamagnetism, ferromagnetism, antiferromagnetism and ferrimagnetism.

Diamagnetism is a property common to all materials and consists in a weak repulsion to the magnetic field. They have negative magnetic susceptibility ($\chi < 0$), that does not change with the temperature. For what concerns **Paramagnetism**, a magnetic field is altered by paramagnetic particles, which can be considered as little magnet interacting with the external field, align with it and amplify it. These materials do not have long range order and are characterized by a small positive magnetic susceptibility. By contrast, the materials in the other two main categories exhibit ordered magnetic moments below the critic temperature (T_c) even without the application of an external magnetic field. **Ferromagnetism**, so called cooperative phenomenon, is typical to those material having aligned atomic magnetic moments of equal magnitude and crystalline structure that allows direct coupling interaction between the magnetic moments, conferring a spontaneous magnetization even with the absence of an applied magnetic field. Materials having atomic magnetic moments of equal magnitude that rearrange in an antiparallel order expose **Antiferromagnetism**: this peculiar order leaves a zero-net magnetization. Finally, **Ferrimagnetism**, as ferromagnetism, is displayed by materials with aligned magnetic moments but with non-parallel arrangement of neighboring sublattices. At a macroscopic scale, the behavior is similar to that of ferromagnetic materials; above the Neel temperature, the substance becomes paramagnetic. [4],[9],[10]

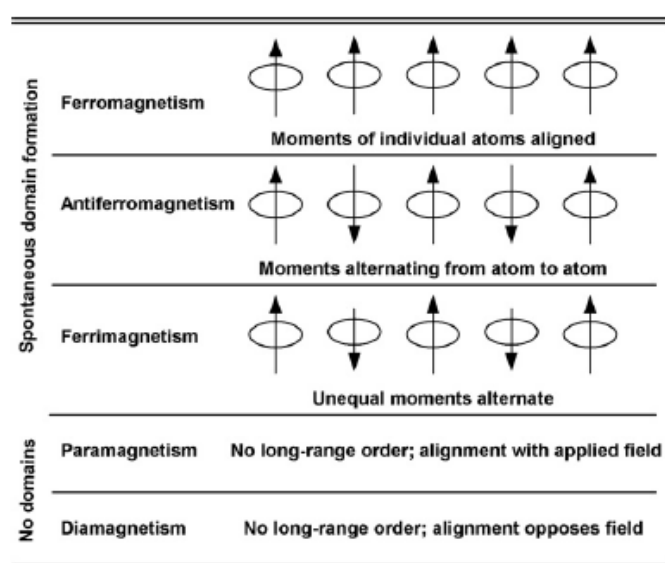


FIGURE 2.7 DIFFERENT TYPES OF MAGNETIC BEHAVIOR[9]

Domains are groups of spins all pointing in the same direction and acting cooperatively. They are separated by domain walls, which have the characteristic width and energy associated with their formation and existence. It has been certified that the coercivity (the magnetic intensity needed to reduce to zero the magnetic flux density of a fully magnetized sample or to demagnetize a magnet) is dependent on the particle size: in particular, the coercivity (H_c) increase with the decrease of the grain size (D), so is proportional to $1/D$. While the magnetic domain moves closer to the grain size, the multidomain material change into a monodomain material, and the coercivity increase quite a lot, because of the impossibility to change the magnetization only by shifting the domain walls.

When the size of the magnetic material reaches 20 nm or less, it assumes a **Superparamagnetic** behavior. In this state, the nanoparticles are aligned in a preferred arrangement, by which they approach to magnetization faster than the other states, since each atomic magnetic moment retains its ordered state leading to a non-hysteretic curve. In other words, although the particle itself is a single-domain ferromagnet, its ability to store magnetization is lost when its dimension is below threshold. Hence, the magnetic moments within a particle rotate rapidly simultaneously, exhibiting the superparamagnetic phenomenon.

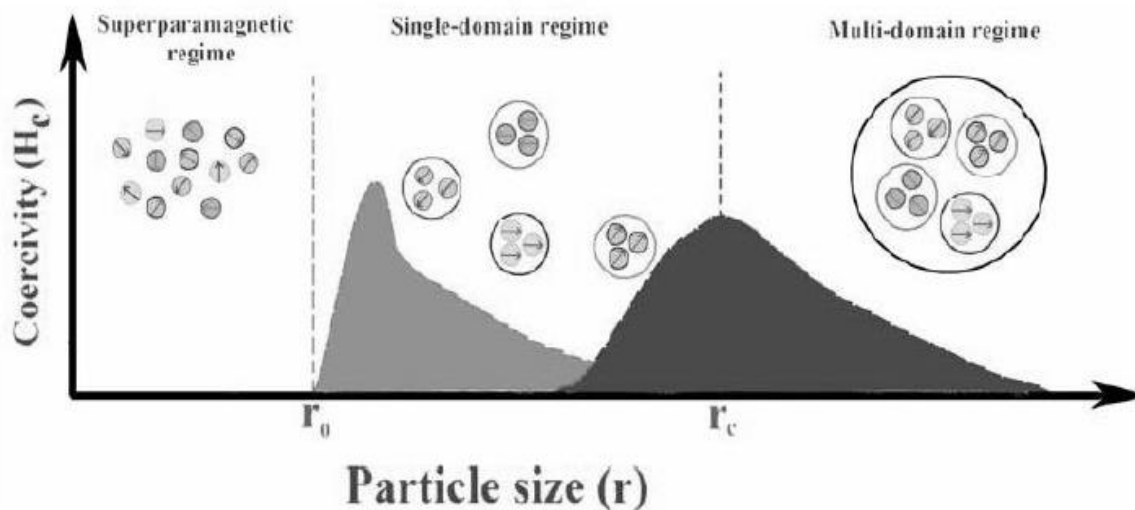


FIGURE 2.8 DEPENDENCE OF COERCIVITY ON A PARTICLE SIZE[11]

The importance of this property becomes clear when we talk about colloids, in which it translates into stability of the suspension. Due to the null or negligible residual magnetization, the colloids are not able to aggregate neither during storage or after administration, even when

the magnetic field is suppressed: they stay paramagnetic, even if the Curie temperature is not reached. [9],[10],[12]

The parameters that characterized magnetic materials are:

- Curie temperature
- Neel temperature
- Temperature of phase transition
- Hysteresis parameters

2.3.2 Principles of magnetic heating

Magnetic hysteresis

The most commonly measured magnetic parameters are schematically illustrated in a hysteresis loop. The application of a sufficiently large magnetic field causes the spins to align with the field itself. The maximum value of the magnetization achieved in this state is called saturation magnetization M_s . While the magnitude of the magnetic field decreases, spins stop to be aligned with it and so decrease the total magnetization. The value of magnetization at zero field, typical of ferromagnetic materials, is called remanent magnetization, M_r . The ratio between them, M_r/M_s , is called the remanence ratio and varies from 0 to 1; finally, the coercive field H_c is the magnitude of the field that must be applied in the negative direction to bring the magnetization of the sample back to zero. [9]

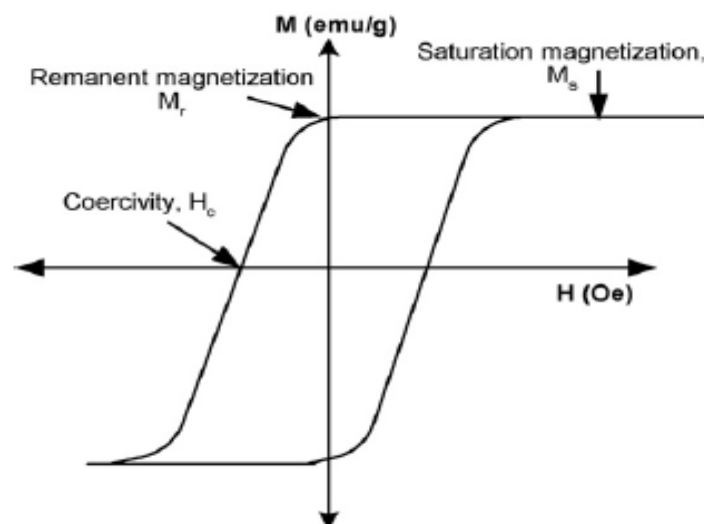


FIGURE 2.9 HYSTERESIS CYCLE OF A MULTIDOMAIN MATERIAL, WHERE H IS THE MAGNETIC FIELD AMPLITUDE AND M THE MAGNETIZATION OF THE MATERIAL [9]

Superparamagnetism and magnetic relaxation

As stated before, Superparamagnetism occurs when ferromagnetic or ferrimagnetic nanoparticles have their diameter below a threshold value of 20 nm. In this state, the particles are considered single-domain ferromagnets without domain walls, they lose the ability to store magnetization and so the typical hysteresis cycle.

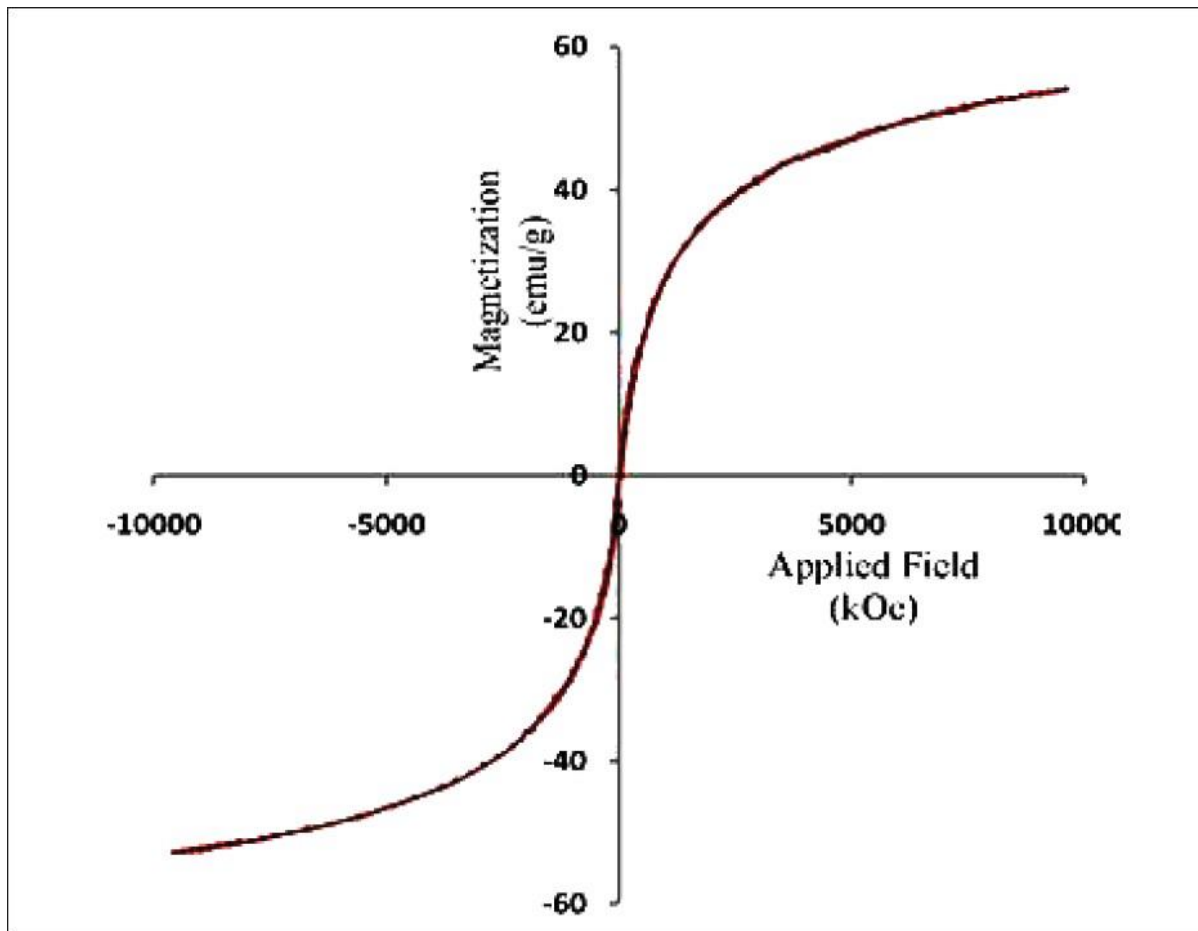


FIGURE 2.10 SUPERPARAMAGNETIC HYSTERESIS LOOP

When the external field is switched off, condition called zero-field, no residual magnetization is left in the nanoparticles: this loss, however, is a non-equilibrium process, which means that it will tend to occur with a typical relaxation mechanism. Generally, in the presence of a such external magnetic field, the rotation of the particle's magnetic moment to align to the field itself requires overcoming an energy barrier, given by $K \cdot V$ for uniaxial particle, where K is the magnetic anisotropy and V the volume of the particle. The relation between this barrier to moment reversal and the characteristic time of thermal fluctuations of the magnetic moment of

a single-domain particle, hence the time needed to establish the thermal equilibrium in a system of single-domain particles, is described by the Neel relaxation time:

$$\tau_N = \tau_0 e^{\frac{KV}{kT}} \quad (4)$$

Where τ_0 is the characteristic flipping time, an expression of the anisotropy energy, and is about 10^{-9} s, being weakly dependent on the temperature, k is the Boltzmann constant and T is the temperature. Since the energy barrier is proportional to the volume, for small particles the thermal activation due to kT causes the flipping of the net moment direction. So, such particle mimics a paramagnetic particle with a huge magnetic moment. [13],[14],[15]

However, another relaxation mechanism may occur, in which the magnetic dipoles respond to a time-varying magnetic field through physical free rotation, termed Brownian relaxation. Because of the Brownian motion in a system of single-domain nanoparticles, also called ferrofluid, its net magnetization will be null, even if each particle performs as a magnet. Hence, when the magnetic field is switched off, the total magnetization reduces to zero.[14],[15]

The relaxation time of this rotation can be approximated by:

$$\tau_B = \tau_0 \frac{3\eta V_h}{kT} \quad (5)$$

Where η is the viscosity of the carrier liquid and V_h is the effective hydrodynamic volume, which can vary from the geometric volume, because of, for instance, adhering layers.

Application of moderate or high magnetic fields may change the magnitude of these relaxation times, but in general the particles will respond to the field either through physical rotation or internal dipole reorientation.

The effective relaxation time of the ferrofluid will be so given by:

$$\frac{1}{\tau} = \frac{1}{\tau_N} + \frac{1}{\tau_B} \quad (6)$$

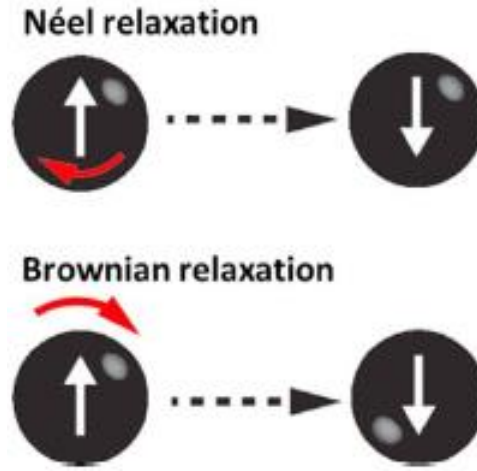


FIGURE 2.11 RELAXATION PROCESSES THAT INFLUENCE THE HEATING PROPERTIES OF MAGNETIC NANOPARTICLES [16]

When the particles are exposed to an AC magnetic field with the time of magnetic reversal less than the magnetic relaxation time of the particles, heat is dissipated due to the delay in the relaxation of the magnetic moment. So the heat dissipation is obtained with the harmonic average of the two relaxation times and their relative contributions depending on the particle diameter.

The heating power during relaxation results from:

$$P(f, H) = \mu_0 \pi f H^2 \chi'' \quad [\text{W/m}^3] \quad (7)$$

where μ_0 is the magnetic field constant, f is the frequency of the magnetic field, χ'' is the magnetic susceptibility (imaginary part) and H is the strength of the field.

By using the Specific Loss Power:

$$SLP = \frac{P}{m} \quad [\text{W/kg}] \quad (8)$$

where m is the mass of the magnetic nanoparticles. [13],[16]

It is notable that, for medical reasons, it is impossible to reach high frequency and large amplitudes of the magnetic field, as it is needed for hyperthermia, so it is quite impossible to reach big SLP.

Finally, the above equations indicate that the Neel time is strongly dependent on the nanoparticle size and the Brownian relaxation time also depends on the hydrodynamic size of the nanoparticle as well as depends on the viscosity of the fluid. Hence, small magnetic

nanoparticles are more appropriate for intracellular hyperthermia because of the requirement of less energy for rotation of magnetic moment and low restriction of nanoparticles rotation in cellular environments of high viscosity. [17]

Magnetic Hyperthermia

Hyperthermia is a minimally invasive procedure which destroys cancer cells by heat generated in alternating magnetic fields by magnetization reversal losses of magnetic nanoparticles applied to a tumor. Different thermotolerance between tumor and healthy cells enhances sensitivity of cancer cells to a simultaneous chemotherapy or radiotherapy. [18]

In detail, at the temperature between 42°C and 45 °C, it has been shown that mechanism of protein and nucleic acid synthesis slowed down; while RNA and protein synthesis resume quickly after removal of the stress agent, DNA does not, because of the protein aggregation and denaturation, which damage DNA synthesis and repair. Moreover, at a temperature exceeding 42°C, the decreased blood flow as consequence of tumor vasculature damage leads to hypoxia and a more acidic cellular environment, which are considered to contribute to the radio- and chemo-sensitization of cancer cells. [19]

On the basis of treated area, three different types are recognized as official treatments:

1. *Local hyperthermia*: is applied with the aim to heat small tumor areas using radio- and micro-waves or ultrasounds, usually at the temperature of 42°C. The tumor site has punctured vessels allowing the nanoparticles to enter the tumor cell by the passive targeting approach according to the particles' properties. Due to the focus heating, there is no detectable effect on the targeting moieties (e.g. antibodies).
2. *Regional hyperthermia*: used for the treatment of a larger and deeply seated tumors, heat is applied using external arrays of antennas/applicators placed around the area of interest, or by regional perfusion using fluids. When regional hyperthermia is used not in combination with other techniques (e.g. chemotherapy), higher temperatures (43°C) are well tolerated for a period of up to 2 h.
3. *Whole-body hyperthermia*: the temperature of the whole body is raised to 41-42°C for about 1 h under anesthesia. Heating achieved with different methods (hot water blankets, hot wax, infrared etc.), as before if used in combination the temperature must be limited and can be used for longer periods.

Magnetic fluid hyperthermia involves dispersing magnetic particles throughout the target tissue and then applying an AC magnetic field of sufficient strength and frequency to cause the particles heating.

It has been stated that Neel relaxation is the prevalent heat generation mechanism in small nanoparticles: this is because, as mentioned above, Brownian relaxation depend on the ability of the particles to rotate freely. This ability is obstructed or even suppressed in media with high viscosity (such as the intracellular environment) or when the nanoparticles are immobilized in tumors.

The nanoparticles are delivered in one of four ways to the tumor:

- a. *Arterial injection*: the fluid carrying the magnetic particles is injected in the arterial supply of the tumor.
- b. *Direct injection*: the fluid is injected directly into the tumor. The particles will be located in the tumor and most of them in the interstitial space, while the minority intracellularly. So, when the magnetic field is applied, most of the heat originates outside the cells. Functionalization with a coating having specific tumor antibodies can increase the NPs retention in the tumor region, which is desirable, as the hyperthermia treatments are often done repeatedly achieve success.
- c. *In situ implant formation*: magnetic nanoparticles embedded in gel are injected into the tumor.
- d. *Active targeting*: delivering via antibody targeting or via external magnetic field gradient (magnetic targeting). For antibody targeting, the NPs are coated with a tumor specific antibody. After their application into the blood vessels, they find the tumor and bind the specifically targeted receptors.

An additional delivering way is the magnetic targeting. After the application of the nanoparticles, an external field gradient close to the tumor tissue leads to a magnetic attraction acting on the NPs circulating in the blood stream and to their magnetic concentration in the tumor tissue. [7],[13] ,[17],[19]

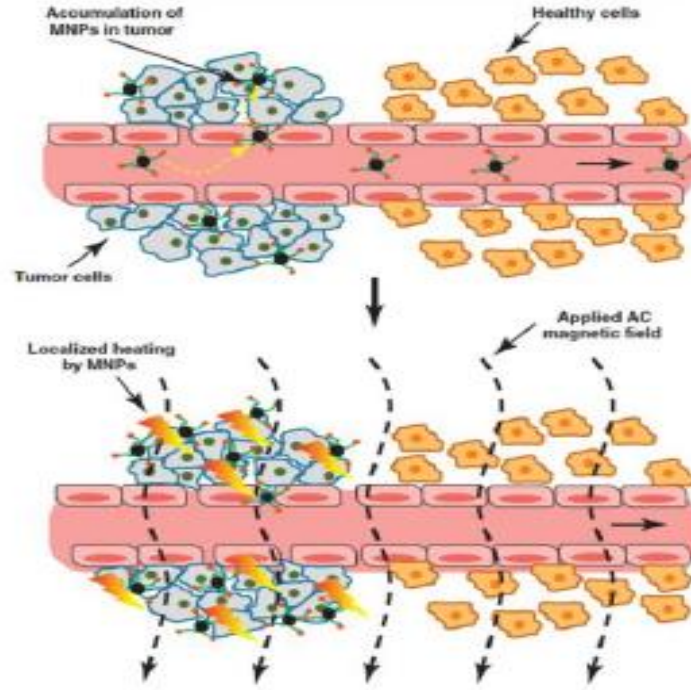


FIGURE 2.12 SCHEMATIC DEPICTION OF MAGNETIC FLUID HYPERTHERMIA. THE UPPER IMAGE SHOWS THE ACCUMULATION OF MAGNETIC NANOPARTICLES IN TUMOR TISSUE (EPR). THE LOWER IMAGE EXEMPLIFIES THAT AFTER THE APPLICATION OF AN AC MAGNETIC FIELD, THE SPIONS IN THE TUMOR HEAT UP AND DAMAGE THE TISSUE.[7]

The Specific Absorption Rate (SAR) is the parameter determining the heating of the tissue; it is addressed as the rate at which electromagnetic energy is absorbed by a unit mass of biological material. It is calculated as:

$$SAR = C \left(\frac{\Delta T}{\Delta t} \right) \left(\frac{m_s}{m_m} \right) \quad (9)$$

where C is the sample specific heat capacity, $\left(\frac{\Delta T}{\Delta t} \right)$ is the increase in temperature over time, m_s is the mass of the solvent and m_m the mass of the magnetic particles.[17],[19]

2.4 Colloidal properties

Magnetic particles can be enumerated among countless biomedical application; in particular, colloidal suspensions of iron oxide particles, called ferrofluids, that possess a unique combination of fluidity and capability to interact with a magnetic field for many purposes.

For biomedical employments, the stability of colloids and the suitability of specific surface coating for prevention of undesirable adhesion are most important factors. [20]

As said, ferrofluids are associated with small, single-domain magnetic particles suspended in a good continuous phase whose rheological behavior can be adjusted using a magnetic field. To control the colloidal stability of ferrofluids, repulsive and attractive forces, such as Van der Waals, steric, hydrophobic and double layers, must be equilibrated: this balance has been evaluated with the so called Derjaguin-Landau-Verwey-Overbeek (DLVO) theory. Thanks to this theory, is possible to forecast the net interactions energy implicating those forces in dilute dispersions.

The stability and fluctuations of these colloids can be controlled by varying the electrostatic charge on particles' surface or changing the ionic properties of the medium: this, for example, can shift the electrostatic repulsions and can led to particles' flocculation in powerful magnetic fields. [21]

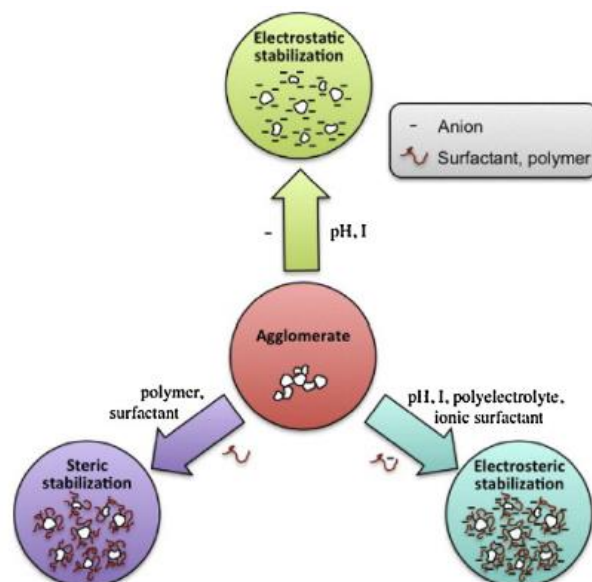


FIGURE 2.13 SCHEMATIC ILLUSTRATION OF MAIN MECHANISMS FOR STABILIZATION OF MAGNETIC NANOPARTICLE DISPERSION [20]

The three principal aggregation forces characterizing SPIONs in water are: hydrophobic-hydrophilic, magnetic and Van der Waals. The first one is responsible for the aggregation due to the high surface force, that is caused also by the dipole-dipole interaction between particles. These aggregates become further magnetized by neighboring clusters, condition that can be worsened by the application of an external magnetic field.

The force that is always present in IONs dispersion and that must be monitored to guarantee an adequately long-range repulsion, and so a stable ferrofluid, is the Van der Waals force. The amount and range of the Van der Waals interactions are directly related to the Hamaker constant, A , which itself is related to the dielectric properties of the implicated materials.

The attraction, for example, between two spheres of radius r at a surface separation s can be so calculated:

$$V_{vdw} = -\left(\frac{A}{12}\right) \left(\frac{r}{s}\right) \quad (10)$$

when $s \ll r$. In a stable system, the thermal energy should be more than once or twice the maximum attractive interparticle energy, so it can easily break all particle-particle bonds.

Hence, it results clear how much a stabilization of the particle in the suspension is important to avoid aggregation. [21]

2.5 Biocompatibility

Upon their *in vivo* administration, the magnetic nanoparticles are, within minutes, challenged by macrophages of the Reticuloendothelial System (RES). The efficacy of particle clearance by the RES depends on various properties of the particle itself and can influence mechanism of macrophage activation and particle internalization. [22]

Hence, it is explicit that for the implementation of a correct therapy with these particles, whose aim is to target the tumor cells while leaving the healthy cells unaffected. Biocompatibility is one of the fundamental properties that have to be reached in order to guarantee a successful application.

While iron oxide is considered safe, imbalance in its homeostasis has toxic implications to many organ systems. It is known that IONs toxicity encompasses the generation of reactive oxygen species (ROS), which causes lipid peroxidation, destroying the membrane and resulting in cell

death: the free iron ions, created by the hydrolysis of ION in lysosomes, are transported to the cytosol, where they undergo a reaction with mitochondrial hydrogen peroxide and form hydroxyl radicals ($\cdot\text{OH}$), a reactive ROS; these radicals easily concentrate in the brain and excess iron is associated with multiple neurodegenerative disorders, including multiple sclerosis, Alzheimer's and Parkinson's disease.

However, it has been tested that, of several magnetic nanoparticles, iron oxide nanoparticles are the safest to be used, producing cytotoxic changes at levels of 100 $\mu\text{g/ml}$ or higher. Furthermore, reduced cytotoxicity changes at levels of IONs is associated with increased particle solubility and modification of surface chemistry.

Coating material are the ones that really interact with the biological environment: doing so, for example, they prevent the adsorption of those plasma proteins sent by the RES, and responsible for the clearance of the particle, and so extend the IONs circulation time in blood and maximize the possibility to reach the target tissues. On the other hand, anyway, the permanence of nanoparticles in the intracellular habitat can have devastating effects on cell morphology, increasing cellular stress and inducing changes in the architecture of the actin skeleton.

Hence, surface coating, along with other physicochemical parameters (e.g. size, concentration, administration route, etc.), are very important factors for cell uptake, as well as the cellular type. It has been shown, for example, that SPIONs having a different surface chemical composition (uncoated and cyanoethyltrimethoxysilane- and aminopropyltriethoxysilane-coated) revealed toxic impacts on human brain cells at iron concentration above 2.25 mM, whereas the same concentration of NPs was acceptable in human kidney. [22],[23],[24]

2.6 Surface coating

As stated before, surface modification of iron oxide nanoparticles is often indispensable. In fact, without any surface coating, particles exhibit hydrophobic interactions, forming articles aggregates and resulting in increased particles size. These clusters, when approaching one another, come into the magnetic field of each one and get further magnetized: these mutual magnetization causes an increased aggregation property.

Furthermore, although iron oxide nanoparticles are in general, less sensible to oxidation, because of the presence of vulnerable Fe^{2+} , they could be oxidized and converted to $\alpha\text{-Fe}_2\text{O}_3$,

which, is known, demonstrate no magnetism. Encapsulation of magnetic nanoparticles, so, makes them less sensible to oxidation, agglomeration and corrosion, granting them the possibility to remain single-domain structures. In addition, it is notable that surface modification of IONs prevents them from being directly exposed to the body, improving their biocompatibility. [11]

Hence, it sounds clear how important is surface modification, which, as said, allow the magnetic nanoparticles to be dispersed into homogeneous ferrofluids and improve their stability. Various coating materials can be used in surface chemistry:

- i. Organic polymers: dextran, chitosan, polyethylene glycol (PEG), etc.
- ii. Organic surfactants: sodium oleate, dodecylamine, etc.
- iii. Inorganic oxides and metals: silica, carbon, gold, silver.
- iv. Bioactive molecules and structures: liposomes, peptides and ligands/receptors.

Organic polymers

Although until now most of the studies focused on surface chemistry involving surfactants, recently polymers used to stabilize magnetic nanoparticles are receiving more attention.

Polymers, in general, can increase repulsive forces more than surfactants and, granting the nanoparticles features like well-defined composite materials and good dispersion, can be adopted in several fields. It has been shown that both synthetic and natural polymers can be attached to the surface of IONs; the most common natural polymers are dextran, chitosan and gelatin, while the synthetic ones are polyethylene glycol (PEG), polyvinyl alcohol (PVA), polylactide acid (PLA). Nevertheless, a thin polymer coating is not very suitable to protect reactive magnetic nanoparticles: they are not air stable and so vulnerable to acidic solution, which causes the loss of their magnetization. In addition, the polymeric nature of the coating is characterized by an intrinsic low stability to high temperatures, enhanced by the catalytic action of the metallic core. [25]

Organic surfactants

On the other hand, a dense coating of organic surfactant is vital for countering the particles from being oxidized by air. [25]

Among all the possible surfactant coating, two are of most interest for this work: citric acid (CA) and 3-aminopropyl-triethoxysilane (APTES).

Citric acid ($C_6H_8O_7$) is a bio-compatible tri-carboxylic acid, that can be absorbed onto the surface of the particle using one or two carboxylate functionalities, leaving at least one of them exposed to be used for further functionalization. Because of its pK_a value (3,13), citric acid will be highly deprotonated to COO^- over the pH range of natural aqueous solutions (5-9); these groups keep the surface highly negatively charged and grant strong electrostatic repulsion, including in quite acid environments. Thanks to this property, the nanoparticles, intrinsically hydrophobic, will become hydrophilic and will be equipped with stability in the solution.

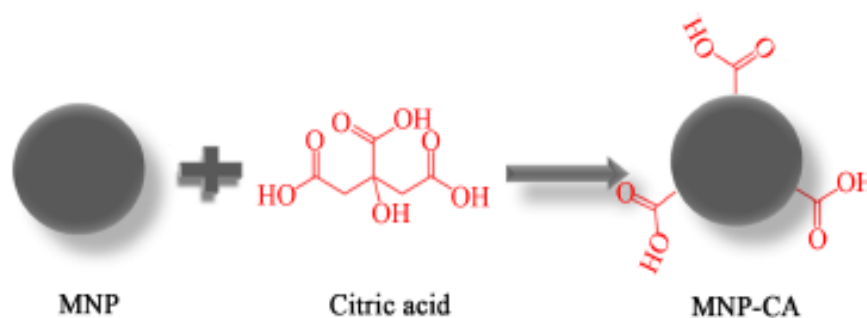


FIGURE 2.14 SCHEME FOR THE FUNCTIONALIZATION OF MAGNETIC NANOPARTICLES WITH CITRIC ACID[26]

As testified by previous studies, the functionalization of iron oxide via CA shows no negative effects: for the small-size nanoparticles (~ 9 nm), the superparamagnetic behavior is not affected by CA, leading only to an increased hydrodynamic size of the coated NPs; moreover, CA-NP are stable in aquatic environment, even over wide ranges of pH and ionic strength.[27],[28]

3-aminopropyl-triethoxysilane (APTES) is an alkoxysilane, the most used to modify the surface of the nanoparticles, via the silanization process (produces via hydrolysis and condensation of the organosilane compound), thanks to its ability to expose its terminal amino groups, used to attach biomolecules, drugs or metals. The concentrations of bioactive molecules on the surface is directly dependent on the number of amino groups exposed, so the control of their concentration is a fundamental step.

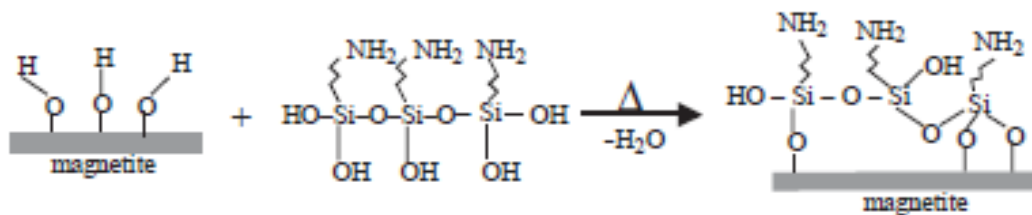


FIGURE 2.15 SCHEME OF SILANIZATION REACTION OF APTES ON THE MAGNETITE SURFACE [29]

Again, previous studies demonstrated that the functionalization with APTES causes the formation of a thin and continuous layer of silane on the surface of the magnetite core, causing a derisory variation of the diameter, but without affecting their magnetic properties. On the other hand, this process can grant high stability and dispersibility in water, basic groups of amino and hydroxy anchored on the surface and a protective layer against mild acid and alkaline environments. [29],[30]

Inorganic oxides and metals

Another simple approach to protect the NPs to oxidation is to equip them with an oxide layer. The first and easier way is to induce a controlled oxidation of the pure metal core, a technique known for the passivation of air-sensitive catalyst: in this way, the iron nanoparticles show the features of both iron oxide and metallic iron, very useful foe further application.

The second one consists in using metal oxides with different natures to the magnetic core (titanium oxide, zirconium oxide, etc.): the surfaces of these oxides are phosphorylated, making them suitable for biological application. [25]

Precious metals, such as gold and silver, are widely used due to their specific surface derivative properties for subsequent treatment with chemicals or biomedical agents. Surface modification with these types of biocompatible metals provides again particle's stabilization and prevent their aggregation and, on the other side enables the incorporation of some optical properties on magnetic nanoparticles, promoting their optical and magnetic diagnosis applications.

Silica and **carbon** are two of the most known inorganic coating agents. Silica shells can guarantee low cytotoxicity, easy tunable surfaces, high stability under water conditions and easy control of interparticle interaction, all through only the variation of the shell's thickness. In addition, thanks to the negative charge in the pH range of 6-7, it can mimic the negative charge of most biomolecules in physiological conditions. Nevertheless, in the case of silica-

coated magnetic, under rigid conditions is nearly impossible to get a dense and nonporous silica coating, making difficult to maintain high stability of NP.

Carbon, besides, is one of the best options to incorporate metal nanoparticles, being more chemically and thermally stable, cheap, light and biocompatible. [11],[25]

In the next chapter, the properties, features and application of gold and silver nanoparticles, attached to IONs, will be discussed in detail.

3. Iron Oxide – Ag/Au Nanocomposites

In the past few years, magnetic nanoparticles have become an emerging solution in biological application, thanks to their biocompatibility and attractive magnetic properties.

As previously said, for high performance applications, magnetite particles must possess a narrow size distribution, smooth surface and other peculiar properties, together with the ability to form colloidal suspensions in physiological fluids. This last feature has been shown to be challenging, because of the tendency of the magnetic nanoparticles to cluster and precipitate. Because of that, the functionalization of the surface of the nanoparticles has been developed quite a lot lately.

Coating with noble metals, such as Silver and Gold, could be an excellent solution not only to prevent aggregation and precipitation of the IONs, but also to grant them enhanced physical and chemical properties. [31]

Hence, a lot of effort is focused on obtaining nanostructures with magnetic and plasmonic features. In particular, iron oxide nanoparticles can be implemented in several technological fields, such as magnetic recording, magneto-optical systems, MRI contrast agents or magnetic hyperthermia. On the other hand, noble metals as Au and Ag, are ideal and attractive materials for deposition, due to their low reactivity, high chemical stability and biocompatibility. Moreover, the presence of metallic content could provide a platform for optical absorption and emission caused by the electronic response of the metal to light, with a well-defined Surface Plasmon Resonance (SPR) peak, which can be shift in a controlled manner by association with a metal oxide.[32],[33]

Different approaches have been developed for the synthesis of iron oxide nanoparticles decorated with Au or Ag nanoparticles. The two main synthesis routes are:

1. Iron oxide core synthesis followed by gold and silver seeding (gold and silver nanoparticles are synthesized separately and then attached onto iron oxide surface).
2. Synthesis and coating of nanoparticles in the aqueous phase, with the iron oxide core synthesized via co.-precipitation method of iron salts in alkaline environment, followed by the direct reduction of chloroauric acid, HAuCl_4 , or silver nitrate, AgNO_3 , on the ION surface (*in situ* reduction) in order to obtain iron oxide – Ag/Au nanocomposites.

3.1 Structure and synthesis of Iron Oxide – Metal Nanocomposite

In general, the of Fe_3O_4 – Ag/Au nanocomposites can be divided into two categories: monodispersed nanoparticles and aggregates. It is noticeable that monodispersed nanoparticles have drawn more attention from chemists and material scientist due to their promising reproducibility and reliable characteristic properties for further modification and applications.[34]

Here are reported the most characteristic nanocomposite structures according to the literature. [31],[33],[34],[35]:

- a. *Core-shell structure*: nanocomposite portrayed by a single core, typically iron oxide, fully coated by a shell of metal, gold and silver in this case. The properties of the nucleus can be reduced by the coating, which, on the other hand, can grant to the nanocomposite enhanced surface properties.
- b. *Nanodumbbells*: characterized by one metal nanoparticles attached to the surface of one iron oxide nanoparticles. They are also characterized by a balanced ratio of Fe_3O_4 and metal and present an increased magnetic anisotropy and blocking temperature compared to bare IONs.
- c. *Nanoflowers*: resembling a flower-like structure, it can be regarded as a multiple dumbbell structure. Composed by a single iron oxide core surrounded by few Ag/Au nanoparticles of similar size. They present an enhancement in blocking temperature and magnetic anisotropy even larger than nanodumbbell structures.
- d. *Aggregates*: random structure, obtain by a random aggregation induced by radiation or via a polymer wrap.

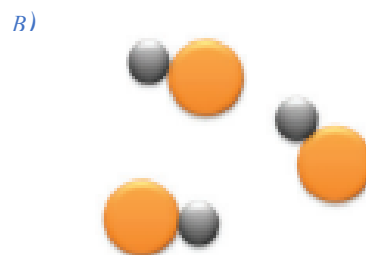
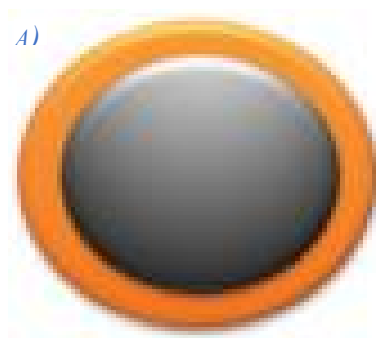




FIGURE 3.1 THE MOST CHARACTERISTIC NANOCOMPOSITE STRUCTURES: A) CORE-SHELL, B)
[34]

To be noticed, as said, a common feature from the presence of silver or gold on the surface of the iron oxide, besides changes in shape and size, is the modification of the optical index, which causes the shifting of surface plasmon resonance peak.

The synthesis of the iron oxide nanoparticles has already been pointed out in the Chapter 2 “Iron Oxide Nanoparticles”, paragraph 2.2 “Synthesis approaches”. For what concerns the synthesis of metal nanoparticles, the different routes can be summarize as follows.

3.1.1 Synthesis of Ag nanoparticles

Silver nanoparticles are synthesized using several approaches, among them chemical, physical and biological are the most popular. Chemical methods use organic solvents or water in order to prepare the nanoparticles. In this process three principal components are involved, such as metal precursors, reducing agents and stabilizing/capping agents. In general, the reduction of silver salts includes the nucleation stage first and, then, the growth stage. This procedure is called “bottom-up”, together with electrochemical method and sono-decomposition; on the other hand, the “top-down” method is a mechanical grinding of the bulk metal with following stabilization with colloidal protecting agents. Physical methods consist in evaporation-condensation using a tube furnace at atmospheric pressure, including spark discharging and pyrolysis. Finally, biological synthesis methods depend on three factors: the solvent, the reducing agent and the material; in this approach several bacteria can be used, such as *Escherichia coli* or *Bacillus licheniformis*, as well as several plant extracts. In addition to these, various biomolecules as biopolymers, starch and amino acids can be used.

Nevertheless, the employment of several reducing agents, granting a higher control on shape, size, energy, time and yield of the synthesized nanoparticles, together with the concern that physical and biological approaches use toxic mechanisms and sophisticated working

conditions, making them costly and vulnerable towards stability, names the chemical synthesis process as the most popular, characterized by high yield and versatility.[36],[37]

3.1.2 Synthesis of Au nanoparticles

As for silver nanoparticles, also gold nanoparticles can be prepared both with a “top-down” or “bottom-up” approach but, because the limited control on shape and size of the NPs that characterized the “top-down” strategy, the “bottom-up” is usually preferred. Furthermore, given that the nanoscale dimensions are strongly altered by the control of size and morphology, and chemical methods offer advantages like simplicity and scalability, for the specified domain, only these chemical methods involving solution-based reduction will be analyzed. [36],[38]

1. *Turkevich method*: introduced by Turkevich in 1951, this method grants the formation of mono-dispersed Au nanoparticles. The HAuCl_4 solution is boiled and the sodium citrate is added rapidly while the solution is vigorously stirred. The color changing of the solution into wine-red indicates that a colloidal suspension is obtained, and the Au nanoparticles size is about 20 nm. The formation of this colloidal gold is possible thanks to the double property of reducing and capping agent of the sodium citrate. [36],[38]
2. *Burst-Schiffrein method*: published in 1994, with this method is possible to create thiolate-stabilized Au nanoparticles. They are stabilized by relatively strong Au-S bonds, with a diameter in the range of 2-5 nm. Fast addition of NaBH_4 and cooled solutions produce small and monodispersed Au nanoparticles. [38]

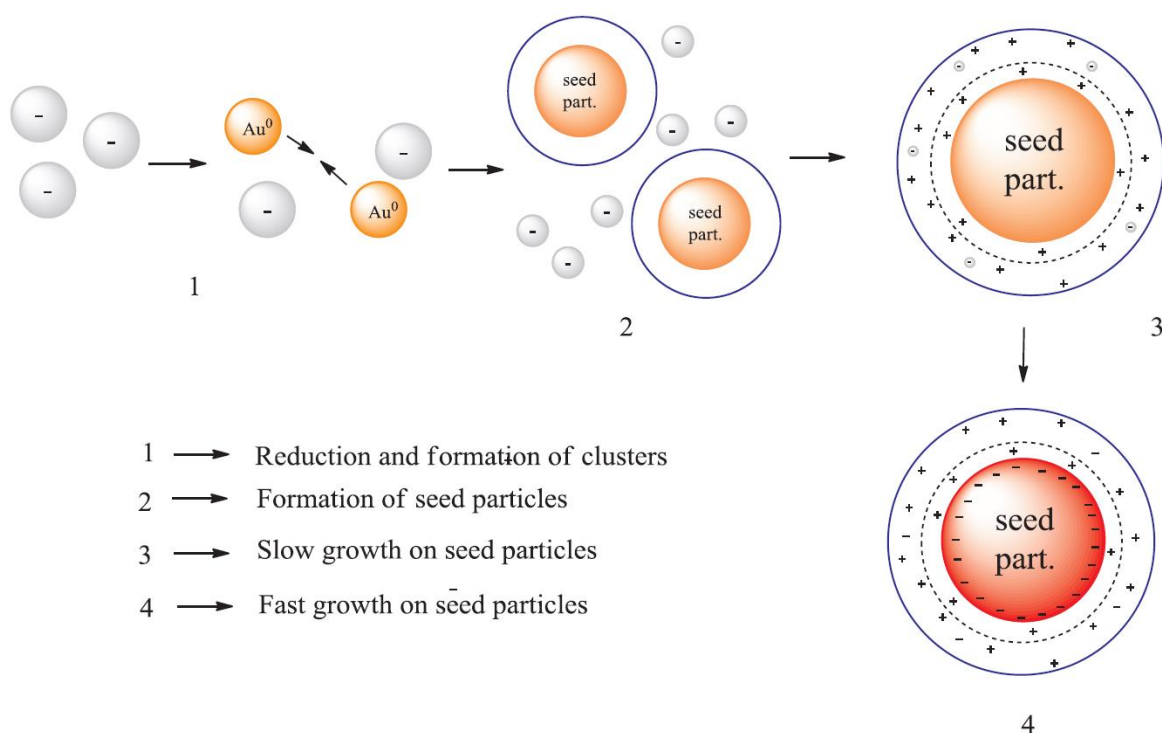


FIGURE 3.2 **GROWTH MECHANISM OF TURKEVICH METHOD**[36]

3.2 Combined magneto-optical properties

Iron oxide – Ag/Au nanocomposites exhibit both magnetic and plasmonic properties due to components combination, making them extremely useful for biomedical application.

In this section the optical, photothermal and sterilizing properties of Au and Ag nanoparticles are described, starting with a short description of the Surface Plasmon Resonance. The magnetic properties of iron oxide nanoparticles are described in the Chapter 2 “Iron oxide Nanoparticles”, paragraph 2.3 “Magnetic properties”.

3.2.1 Surface Plasmon Resonance

When a metal particle is exposed to the magnetic oscillating field of the light, a collective coherent oscillation of the free electrons (conduction band electrons) of the metal is induced. This oscillation around the surface of the nanoparticles produces a charge separation with respect to the ionic lattice, forming dipole oscillation along the direction of the electric field of the light.

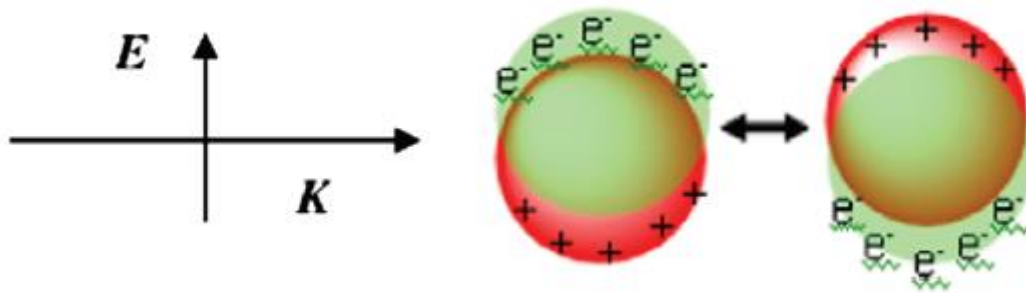


FIGURE 3.3 SCHEMATIC ILLUSTRATION OF SURFACE PLASMON RESONANCE IN PLASMONIC NANOPARTICLES[39]

The amplitude of the oscillation reaches a maximum at a certain frequency, called Surface Plasmon Resonance (SPR): it causes a strong absorption of the incident light and therefore it can be measured using a UV-vis spectrometer. Several factors, such as metal type, particle size, shape, structure, composition and dielectric constant of the surface, which affect the electron charge density on the particle surface, are directly related to the SPR band and wavelength as well. To be noticed, the SPR is much stronger for plasmonic nanoparticles, that is noble metals, especially Ag and Au. [39]

While passing through matter, the energy loss of electromagnetic wave splits in two contributions: absorption, which occurs when the photon energy is dissipated because of inelastic processes, and scattering, when the photon energy causes the oscillation of the electron which emits photons as scattered light. This second emission can be at the same frequency of the incident light (Rayleigh scattering) or at a shifted one (Raman scattering).

Because of the SPR oscillation, the light absorption and scattering are strongly enhanced. The Surface Plasmon Absorption and Resonance are analyzed using the Mie theory. [39],[40]

3.2.2 Mie Theory

Several approaches have been presented to solve the problem of the interaction between light and nanostructures and, among them, the most popular is the one published by Mie. The problem was considered as a scattering light one.

The method divides the issue in two parts: the electro-magnetic one, that can be solved completely, and the material one, dependent on the determination of the dielectric constant $\epsilon(\omega, R)$, which depends on the radius of the particles as well. The scattering approach, for

particles smaller than 20 nm, leads to the following expression for the cross section C_{ext} , which explain quantitatively the SPR

$$C_{ext} = \frac{24\pi^2 R^3 \varepsilon_m^{\frac{3}{2}}}{\lambda} \frac{\varepsilon_i}{(\varepsilon_r + 2\varepsilon_m)^2 + \varepsilon_i^2} \quad (1)$$

where λ is the wavelength of the incident light, ε_r and ε_i are the real and imagery part of the dielectric function of the metal, ε_m is the dielectric function of the surrounding medium, which is related to its refractive index by $\varepsilon_m = n_m^2$. The real part of the constant of the metal determines the SPR peak position, while the imagery one its bandwidth.

The extinction cross-section is maximized when the denominator in equation NR is minimized, a condition that is guaranteed when $\varepsilon_r = -2\varepsilon_m$, which explain the dependence of the SPR extinction peak on the surrounding environment. For example, for gold particles in water ($\varepsilon_m \approx 1.7$), the expected wavelength is about 520 nm in the visible region.

Gold, silver and copper nanoparticles show strong SPR bands in the visible region, while other metals show weak and broad peaks in the UV region. [39],[40]

3.3 Application of iron oxide-Ag/Au nanoparticles

Iron oxide and noble metals nanocomposites are very attractive materials for biological and medical areas, thanks to their theranostic properties, involving also hyperthermia and MRI.

With the advance in nanotechnology, several solutions emerged, involving disease diagnosis at an early stage, monitoring and treating of these diseases with minimal damage to healthy tissues.

3.3.1 Theranostic: Hyperthermia

As said in Chapter 2 “Iron oxide nanoparticles”, paragraph 2.3.2 “Principles of magnetic heating”, hyperthermia is that process involving heating of tumor cell to cure the disease. Cell death can occur when the temperature of the cellular environment rises above 42°C, hence apoptosis can take place between 41°C and 47°C, while necrosis will begin to take place upon

50°C hyperthermia can be achieved using radiofrequency, microwave and laser, introducing a probe into the body.

Fe₃O₄ and Au/Ag nanoparticles are perhaps the most suitable candidates for creating a hostile environment for tumor cells. Their hyperthermia mechanism can be divided into two general categories: magnetic-induced hyperthermia, for iron oxide nanoparticles, and photo-induced hyperthermia, for silver and gold nanoparticles.

Magnetic-induced hyperthermia

As already said in the previous chapter, magnetic heat would be induced due to the Brownian relaxation, which refers to the friction from total particles oscillation, and Neel relaxation, which refers to the rotation of the magnetic moment with oscillation of each magnetic field.

This heat generated from the nanocomposites is higher than that generated from iron oxide nanoparticles alone: this enhancement is related to a higher magnetic anisotropy of the magnetic fraction with the Ag/Au nanoparticles and higher heat capacity of these noble metals, along with increased blocking temperature in comparison with bare Fe₃O₄ nanoparticles. [33]

In conclusion, although both nanocomposites and pure IONs can achieve magnetic-hyperthermia for cancer therapy, nanocomposites are characterized by a less agglomeration under magnetic field.

Photo-induced hyperthermia

As for the photo-thermal treatment, gold and silver nanoparticles can convert almost 100% of adsorbed light into heat via non-radiative properties. The iron oxide of the hybrid systems provides improvement of the optical response, such as increasing the tuning range or the light scattering; hence, these nanocomposites are characterized by shifted SPR peaks, which grant them the possibility to be sensitive to the NIR region, where blood and tissues are maximally transmissive. Furthermore, found a good balance in the ratio Fe₃O₄ : Ag/Au, the plasmonic constituent will not affect the magnetic properties and so further applications. Hence the parameters to be applied to the laser for the treatment with these nanocomposites are usually similar to those for the metal nanoparticles alone.

Although there still are some limitations to this technique, particularly for treatment of deep seated tumors (as a laser cannot penetrate much centimeters in soft tissues), it should be noticed

that Fe_3O_4 – Ag/Au nanocomposites enable therapy with simultaneous imaging, avoiding damage of healthy tissues, enable enhanced cell targeting for tumor with better stability in the body and, finally, enable to reduce field frequency required for magnetic-induced hyperthermia. [35],[39],[41]

4. Materials and methods

This chapter is focused on materials, methods and techniques used during the experimental session. In the first paragraph all the reagents used are mentioned, while in the second one the experimental routes adopted to optimize the synthesis of SPIONs functionalized with silver and gold nanoparticles are described. Finally, the various techniques used to characterize the samples are delineated.

4.1 Materials

Ferric Chloride hexahydrate ($\text{FeCl}_3 \cdot 6\text{H}_2\text{O}$) in powder, Ferrous Chloride tetrahydrate ($\text{FeCl}_2 \cdot 4\text{H}_2\text{O}$) in powder, citric acid monohydrate ($\text{C}_6\text{H}_8\text{O}_7 \cdot \text{H}_2\text{O}$) in powder, ammonium hydroxide (NH_4OH), (3-aminopropyl) triethoxysilane (APTES), tannic acid ($\text{C}_{76}\text{H}_{52}\text{O}_{46}$), Chloroauric acid (HAuCl_4), Nitric acid (HNO_3), and absolute ethanol were obtained from SIGMA-ALDRICH[®] without modifications. Silver nitrate (AgNO_3) in powder were purchased from PANREAC[®] and used without modifications. Bi-distilled water was used as a solvent for all synthesis steps: it was obtained under a laminar flux suction cabinet with filter HEPA (*High Efficiency Particulate Air Filter*) and carbon active filter.

4.2 Methods

This project has been divided in two main routes. Each step has been optimized in order to obtain a simple and fast way to synthesize SPIONs and to functionalize them with metal (gold or silver) nanoparticles using tannic acid, therefore reaching a good device for further *in vitro* and *in vivo* applications.

First route

1. Synthesis of iron oxide nanoparticles via co-precipitation method;
2. Stabilization in water with citric acid;
3. Functionalization with amino group by APTES;
4. Local synthesis of metal nanoparticles (gold or silver) on magnetite surface (*in situ*) by tannic acid reduction.

Second route

1. Synthesis of iron oxide nanoparticles by co-precipitation method;
2. Stabilization in water with tannic acid;
3. Local synthesis of metal nanoparticles (gold or silver) on magnetite surface (*in situ*) by tannic acid reduction.

4.2.1 First route

Synthesis of iron oxide nanoparticles

Magnetite nanoparticles (Fe_3O_4) were synthesized by the co-precipitation method in aqueous medium of Fe^{2+} and Fe^{3+} ions after the addition of ammonium hydroxide NH_4OH .

According to the literature[42], solution of ferrous chloride $\text{FeCl}_2 \cdot 4\text{H}_2\text{O}$ (0.1 M) and ferric chloride $\text{FeCl}_3 \cdot 6\text{H}_2\text{O}$ (0.1 M) were used.

In order to obtain solutions 0.1 M in 50 ml of water, the final amount of salts required was achieved knowing their molecular weight:

$$n(\text{FeCl}_2) = 0.05 \text{ l} * 0.1 \frac{\text{mol}}{\text{l}} = 0.005 \text{ mol}$$

$$M_w(\text{FeCl}_2) = 126.6 \frac{\text{g}}{\text{mol}}$$

$$g(\text{FeCl}_2) = 0.005 \text{ mol} * 126.6 \frac{\text{g}}{\text{mol}} = 0.6334 \text{ g}$$

The used reagent is hydrated, $\text{FeCl}_2 \cdot 4\text{H}_2\text{O}$, so, considering the new molecular weight $M_w(\text{FeCl}_2 \cdot 4\text{H}_2\text{O}) = 198,6 \text{ g/mol}$, the final amount of iron salt is:

$$g(\text{FeCl}_2 \cdot 4\text{H}_2\text{O}) \approx 1.02 \text{ g}$$

The final amount of the other salt, iron tri-chloride hexahydrate ($\text{FeCl}_3 \cdot 6\text{H}_2\text{O}$), was calculated in the same way, resulting in

$$g(FeCl_3 \cdot 6H_2O) \approx 1.3 \text{ g}$$

The required amounts were dissolved each in 50 ml of bi-distilled water, mixed separately with a magnetic stirrer to reach the complete dissolution of the salts. Then 37.5 ml of $FeCl_2 \cdot 4H_2O$ were mixed in 50 ml of $FeCl_3 \cdot 6H_2O$, reaching a pH value around 1.9; under stirring, NH_4OH was added drop by drop to the solution, until the pH reached the range of 9.5-10. The reaction mixture turned black, indicating the formation of the iron oxide nanoparticles.

Afterwards, the suspension was sonicated for 20 minutes and washed several times with bi-distilled water. Sedimentation of the particles was induced by a magnet under the becker, in order to wash SPIONs and so to remove all the unreacted compounds and the residual ammonia. The obtained SPIONs were then resuspended in 100 ml of bi-distilled water.

Stabilization in water with citric acid

As mentioned in the previous chapters, it is fundamental a stabilization step during the synthesis of iron oxide nanoparticles, that prevents their agglomeration and promotes their stability in the solution. To reach this steadiness, citric acid was chosen as stabilizing agent.[43]

First, 50 ml of magnetite solution was separated by sedimentation with a magnet from most of the water, then 60 ml of 0.05 M citric acid solution were added. The pH was, therefore, adjusted to 5.2 with concentrated NH_4OH drop by drop.

The suspension was heated and stirred in an orbital shaker (80 °C, 150 rpm) for 90 minutes. Subsequently, an ultrafiltration device was adopted to wash the particles (3 cycles of 50 ml of bi-distilled water), and finally resuspended in 60 ml of water. The pH of the final suspension was adjusted to 10.2 with ammonia inducing the de-protonation of the -COOH terminal groups of the acid and providing a high, negative surface charge on the nanoparticles, thus preventing any strong agglomeration.

Functionalization with amino group by APTES

As it is known from the literature [29],[30], functionalization with (3-aminopropyl) triethoxysilane (APTES) introduces on the surface of the particles terminal amino (-NH₂) groups; this functional groups are available for many purposes, such as, in this case, immobilization of gold/silver nanoparticles.

For this step of the process, 10 ml of the magnetite solution were dispersed in 150 ml of absolute ethanol. After that, 85 μ l of APTES was added to the colloidal suspension and then heated in orbital shaker at 80 °C for three hours at 150 rpm. Therefore, after it cooled down at room temperature, it was washed several time to remove all the remnant ethanol and finally redisperses in 10 ml of bi-distilled water. To complete the washing procedure, the suspension was centrifugated 3 times, at 7500 rpm for 10 minutes: the final product was diluted in 30 ml of bi-distilled water. To induce positive charge on the surface of the functionalized particles, diluted HNO_3 was added until reaching a pH value ≈ 5 .

Local synthesis of metal nanoparticles

In both routes of this project, silver and gold nanoparticles were prepared through a simple aqueous method with tannic acid as a reducing and stabilizing agent. As it is known from the literature[44],[45], gallic acid has already been used as an excellent stabilizing and reducing agent also thanks to its antimicrobial, antioxidant and anticancer activities. Nevertheless, at alkaline pH, gallic acid induce formation of metal nanoparticles rapidly at room temperature, but its poor stabilization potential leads to aggregation of the particles in solution. On the other hand, tannic acid, under mild acidic/basic conditions, can partially hydrolyze into glucose and gallic acid: the presence of the glucose guarantee the property of being a good stabilizing agent at alkaline pH.

Tannic acid is one of that organic compounds characterized by both hydroxyl and phenolic groups, which grant it aggressive reducing power and take part in redox reactions by forming quinones and donating electrons.

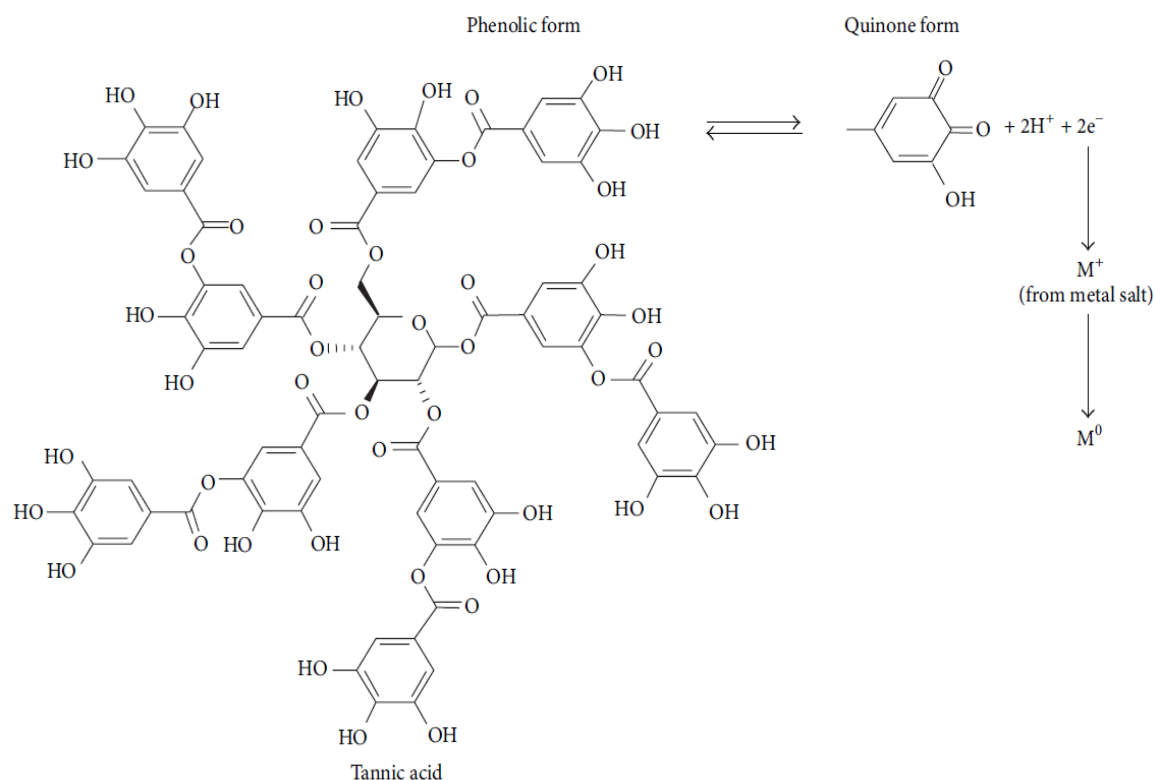


FIGURE 4.1 REACTION MECHANISM OF TANNIC ACID-BASED REDUCTION OF METAL SALTS. THE ELECTRONS RELEASED FROM THE PHENOLIC GROUPS REDUCE THE METAL IONS.[46]

Noticeable, finally, are tannic acid's antioxidant, antimutagenic and anticarcinogenic properties.[46],[47]

Therefore, in this work tannic acid has been chosen as reducing and stabilizing agent:

-Synthesis of iron oxide/gold nanoparticles

To be able to reduce Au nanoparticles onto the iron oxide nanoparticles' surface, 1.685 mg of HAuCl_4 were dissolved in 6.7 ml of bi-distilled water and then added to 10 ml of APTES-coated magnetite nanoparticles; the compound was left in orbital shaker for 5 minutes, 150 rpm, 70 °C. By adding the gold salt into a basic environment, HAuCl_4 hydrolysis takes place and forms gold hydroxide ($\text{Au}(\text{OH})_3$) suspension. To reduce the as obtained $\text{Au}(\text{OH})_3$ ions on the iron oxide nanoparticles surface, 15 mg of tannic acid were dissolved in 10 ml of bi-distilled water, buffered with NH_4OH and, then, added to the solution. The suspension was heated at 70 °C into the orbital shaker for 5 minutes at 150 rpm and then washed three times with an ultrafiltration device and redispersed in 40 ml of bi-distilled water.

-Synthesis of iron oxide/silver nanoparticles

In this case, the precipitation of silver nanoparticles was accomplished in the same way of the gold nanoparticles, still with some variations.

On first, 2.5 mg of tannic acid were dispersed in 20 ml of bi-distilled water and the pH was adjusted to 8; then it was added to 10 ml of APTES-coated magnetite nanoparticles. Therefore, 5 mg of AgNO_3 were dissolved in 10 ml of water and poured into the solution. Finally, the aqueous suspension was then washed three times with an ultrafiltration device and redisperses in 40 ml of bi-distilled water.

4.2.2 Second route

This section is focused on the second method adopted for the synthesis and functionalization of nanoparticles, characterized by tannic acid used as stabilizing, capping and reducing agent. To be noticed, all the syntheses were carried out rapidly, in order to avoid the aggregation of the iron oxide nanoparticles.

Synthesis of iron oxide nanoparticles

As in the first fabrication route, the nanoparticles were obtained by co-precipitation method in aqueous solvent of ferrous and ferric ions after the addition of NH_4OH .

Briefly, 1.02 g of $\text{FeCl}_2 \cdot 4\text{H}_2\text{O}$ and 1.3 g of $\text{FeCl}_3 \cdot 6\text{H}_2\text{O}$ were dissolved each in 50 ml of bi-distilled water. Then, 37.5 ml of the solution of FeCl_2 was poured into 50 ml of FeCl_3 and, under stirring, NH_4OH were added drop by drop until reaching a pH range of 9.5-10. The suspension was, hence, ultrasonicated for 20 minutes and washed several times by using a magnet to induce the NPs sedimentation. After the washing procedures, the particles were suspended in 100 ml of water.

Stabilization with tannic acid and local synthesis of metal nanoparticles

-Stabilization and synthesis of gold nanoparticles

At the beginning, 0.6 g of tannic acid were dissolved in 37.5 ml of water and then the pH adjusted to a value of 8 by adding NH_4OH drop by drop. Then, this solution was added to 25 ml of the magnetite solution and left in orbital shaker for 30 minutes (40 °C, 150 rpm). Afterward, 1.685 mg of HAuCl_4 , dissolved in 6.7 ml of bi-distilled water, was poured to the suspension and left at 70°C in orbital shaker for 5 minutes (150 rpm). Finally, the solution was washed several times through magnetic separation and redisperses in 50 ml of water.

-Stabilization and synthesis of silver nanoparticles

First, 0.6 g of AgNO_3 salt were directly added to 12.5 ml of magnetite solution and sonicated for 15 min at 37°C to prevent aggregation. Then, 0.3 g of tannic acid were dissolved in 10 ml of bi-distilled water and tamponated to pH=8 with NH_4OH . The solution was kept in ultrasound device for 15 minutes at 40°C and then washed with magnetic separation. Again, the nanoparticles were dissolved in 50 ml of water.

4.3 Characterization techniques

In this work the nanoparticles were characterized using traditional techniques:

- I. *Size and morphology*: Transmission Electron Microscopy (TEM), Scanning Transmission Electron Microscopy (STEM), DLS;
- II. *Structure and elemental analysis*: Fourier Transform Infrared spectroscopy (FTIR), Energy Dispersive X-ray Spectroscopy (EDS);
- III. *Magnetic, optical, thermal properties and hemotoxicity*: Ultraviolet-visible spectroscopy (UV-vis), Vibrating Sample Magnetometer, Inductively Coupled Plasma mass spectrometry (ICP-MS), laser.

A brief description of these analytical techniques follows below.

Transmission electron microscopy (TEM)

TEM is used to determine the morphology and the size of the nanoparticles. In transmission electron microscopy, the electron beam passes through the samples and the outer beam is analyzed, after its interaction with the specimen. So, the electron that are actually transmitted are utilized to create the image, after being magnified and focused onto an imaging device (fluorescent screen) or detected by a sensor. The electrons are emitted from a tungsten filament and then deviated with a magnetic field onto the sample, placed on a small gridded disc. All the process and analysis are performed under vacuum.

Samples for the TEM analysis were prepared by adding a drop of NPs suspension on a holey carbon coated TEM grid (300-mesh, S147-3, Agar Scientific, UK). Morphology and size of the prepared samples were characterized using a transmission electron microscope (Jeol JEM-2100) operating at 200 kV for IO NPs equipped with EDXS (Energy-dispersive X-ray spectroscopy) and SAED (selected area diffraction).

Energy dispersive X-ray spectroscopy (EDS)

This technique is performed for elemental analysis and chemical characterization of the sample. It is based on the interaction between X-rays and the sample's electron, resulting in unique peaks in the X-ray spectrum. The electron beam is focused on the sample, whose electrons are unexcited. The beam, then, excite an inner electron to be displaced, which leaves an energy gap. The atom, therefore, is in an excited status and can return to the ground state only if another electron, from a more external shell, occupies the vacancy. At that moment, an X-ray is released, with energy equal to the distance between the two bands: this, because of the characteristic distance and, so, crystalline structure of each elements, allows the measurement of the chemical composition of the specimen.

Scanning Transmission Electron Microscopy (STEM)

The STEM forms a focused beam of electrons that is scanned over the sample while some desired signal is collected to form an image. Thin specimens are used so that transmission modes of imaging are also available. secondary or backscattered electrons can be used for imaging in STEM; but higher signal levels and better spatial resolution are available by

detecting transmitted electrons. A bright field (BF) detector includes the transmitted beam and so the holes appear bright, whereas a dark field (DF) detector excludes the transmitted beam and holes appear dark. Each detector provides a different and complementary view of the specimen. Samples for the STEM (Zeiss supra 40 GEMINI Field Emission Scanning Electron Microscopy) analysis were prepared by adding a drop of NPs suspension on a holey carbon coated STEM grid.

Fourier transform infrared spectroscopy (FT-IR)

Used to detect IR-responsive molecules in matter, it originates from the mathematic process used (Fourier transform) to obtain actual spectrum from raw data. Part of the IR radiation which traverses the sample is absorbed: the resulting spectrum represents the molecular absorption and transmission, creating a molecular identification of the sample itself. It is known that chemical bonds vibrate at a characteristic frequency, derivating from their own structure, bond length and angle: therefore, individual molecules are able to interact with the radiation absorbing it at a specific wavelength. Hence, individual absorption peaks can be associated to individual chemical bonds and, then, used to identify individual compounds in a complex system. The samples were prepared by leaving a small quantity of the solutions to dry in an incubator for 24-48 h. The powder was, then, collected and analyzed with a JASCO 4000 Fourier Transform Infrared Spectroscopy.

Ultraviolet-visible spectroscopy (UV-vis)

This kind of technique analyzes the electronic transitions (in ultraviolet and visible regions of electromagnetic spectrum, 200-700 nm), which is the electron transition from a lower orbital to a higher one after a molecule absorbs energy from UV or visible light. It allows to determine the wavelength and maximum absorbance of compounds.

This analysis, performed with a PerkinElmer Lambda 950 spectrometer, determined the absorption peak and optical properties of the iron oxide – gold/silver nanocomposites, their Surface Plasmon Resonance. All the samples were analyzed in spectrometer-compatible cuvettes, where it was poured approximately 2 ml of the solution.

Vibrating sample magnetometer (VSM)

With this technique is possible to determine the magnetic properties of a material, as functions of magnetic field, temperature and time. The sample, first magnetized with a magnetic field, undergoes a further magnetization by a stray field, which changes with the movement of the sample as a function of time and is sensed by pick-up coils. The alternating magnetic field creates an electric field in the coils proportional to the magnetization of the sample. The system can tell, hence, how much the sample is magnetized and how much of this magnetization depends on the strength of the constant magnetic field.

DLS

For the hydrodynamic size measurements on the water suspensions of NPs ZetaPALS (Brookhaven Instruments Corporation, U.S.A.) was used. The samples were analyzed in cuvettes containing 2 ml of each solution.

Inductively Coupled Plasma mass spectrometry (ICP-MS)

This technique is based on the ionization of the samples with inductively coupled plasma and then using a mass spectrometer to separate and quantify those ions. Thanks to this, it is capable to detect different metals and several non-metals.

In this work, the total concentrations of Fe, Au and Ag in the analyzed samples were determined with the use of mass spectrometry with inductively coupled plasma (ICP-MS, Agilent 7700 ICP-MS instrument, Agilent Technologies, Tokyo, Japan). Stock solutions of Fe, Au and Ag, all obtained from Merck (Darmstadt, Germany), were diluted with water for the preparation of fresh calibration standard solutions. For the determination of the Fe, Au and Ag concentrations in an aqueous suspension of NPs, to a 0.5 mL of NPs suspension 1.5 mL of hydrochloric acid (30 % HCl, suprapure) and 0.5 mL of nitric acid (65 % HNO₃, suprapure) were added. The sample was heated on a hotplate (C-MAG HP10, IKA, Germany) at 100 °C for 10 min until the solution become yellow. After the digestion, the sample was filled up with MilliQ water to a final volume of 10 mL and appropriately diluted prior to the ICP-MS measurements. Digestion was performed in duplicate.

Laser

Samples with total volume of 1 mL were irradiated using NIR laser with a wavelength of 808 nm (CNI, model FC-808). Spot size of the laser beam was 1 cm in order to irradiate the entire volume of the vial. Power of the laser was set in the range of 1 W Irradiation time was 10 minutes. Temperature of the samples was monitored in real time using a J-type Teflon thermocouple.

5. Results and Discussions

This section deal with the results and discussions regarding the experimental work.

The aim of this project was to find an easy and reproducible method to synthesize magneto-optical nanocomposites utilizing tannic acid as reducing agent. Furthermore, the project was divided into two main routes, aiming to obtain the attachment of Au/Ag nanoparticles on the surface of the iron oxide nanoparticles employing different stabilizing agents.

5.1 Size and morphology

5.1.1 First synthesis route

The first route involved the reduction of both HAuCl_4 and AgNO_3 onto the surface of ION, functionalized with Citric Acid and (3-aminopropyl)triethoxysilane (APTES), via tannic acid; these syntheses were performed according to the procedures explained in the previous Chapter. The TEM images (Figure 5.1, Figure 5.2) show the morphology of the obtained samples: a mixture of magnetite and noble metal nanoparticles. Au/Ag nanoparticles are recognizable as the particle with darker contrast.

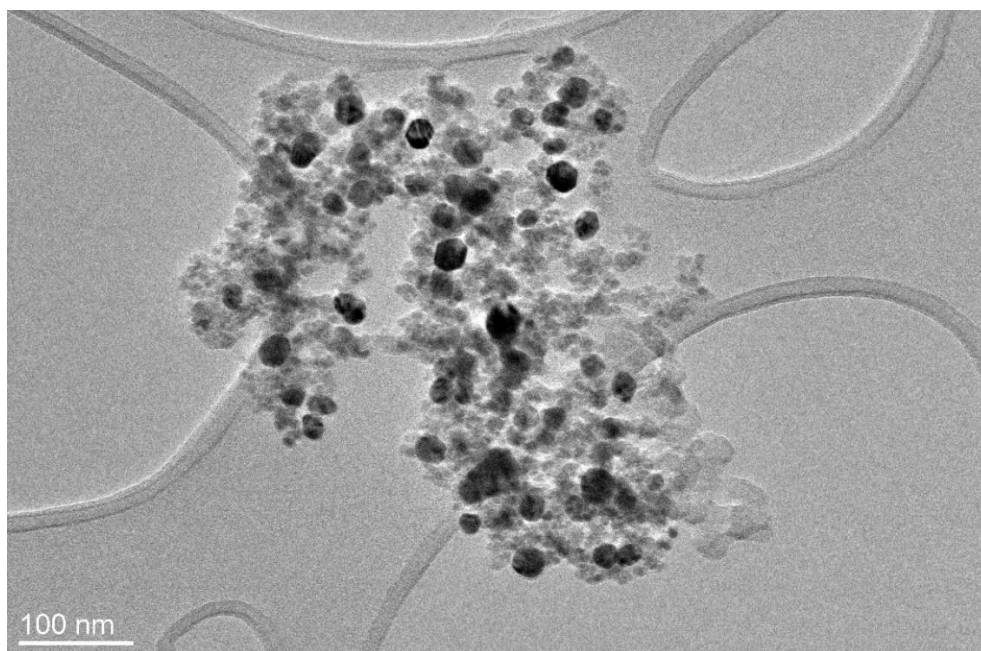


FIGURE 5.1 TEM ANALYSIS OF MAGNETITE NANOPARTICLES (AC+APTES) AND SILVER NANOPARTICLES REDUCED VIA TA

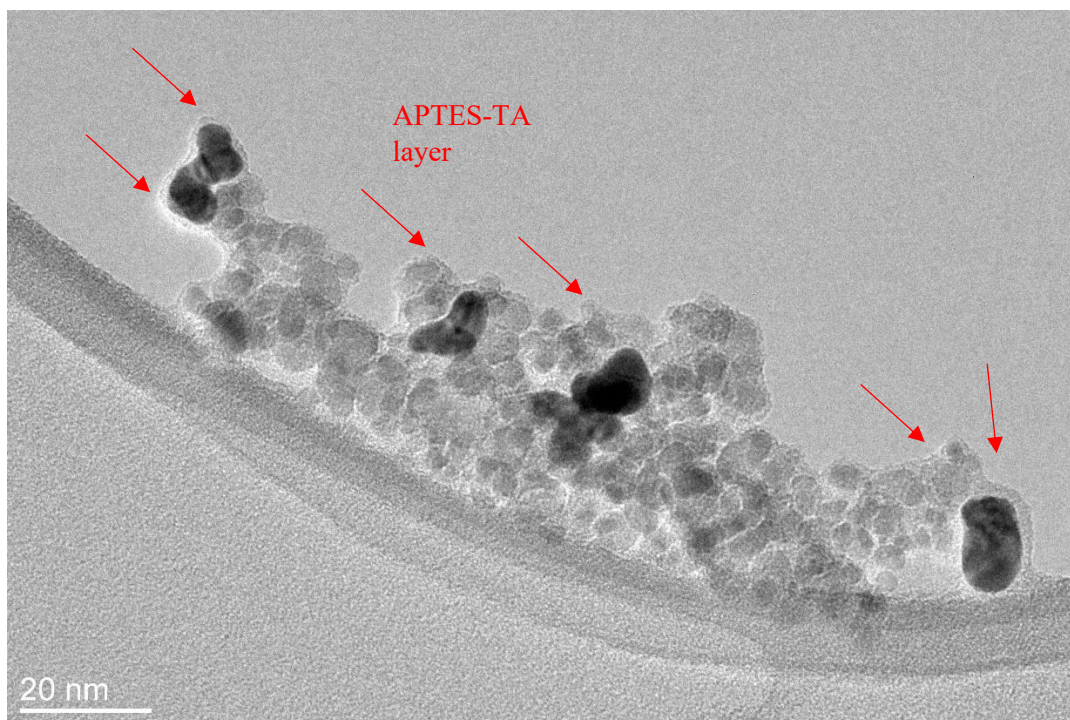


FIGURE 5.2 TEM ANALYSIS OF MAGNETITE NANOPARTICLES (AC+APTES) AND GOLD NANOPARTICLES REDUCED VIA TA

Magnetite nanoparticles show spherical shape with an overall dimensional range of $\sim[5-15]$ nm. However, as seen in Figure 5.1, 5.2 and 5.5, the magnetite nanoparticles are slightly aggregating, because of the preparation of the TEM samples: the samples, as previously said, were prepared by placing a drop of solution onto the TEM carbon coated copper grid, leaving them to dry on a filter paper.

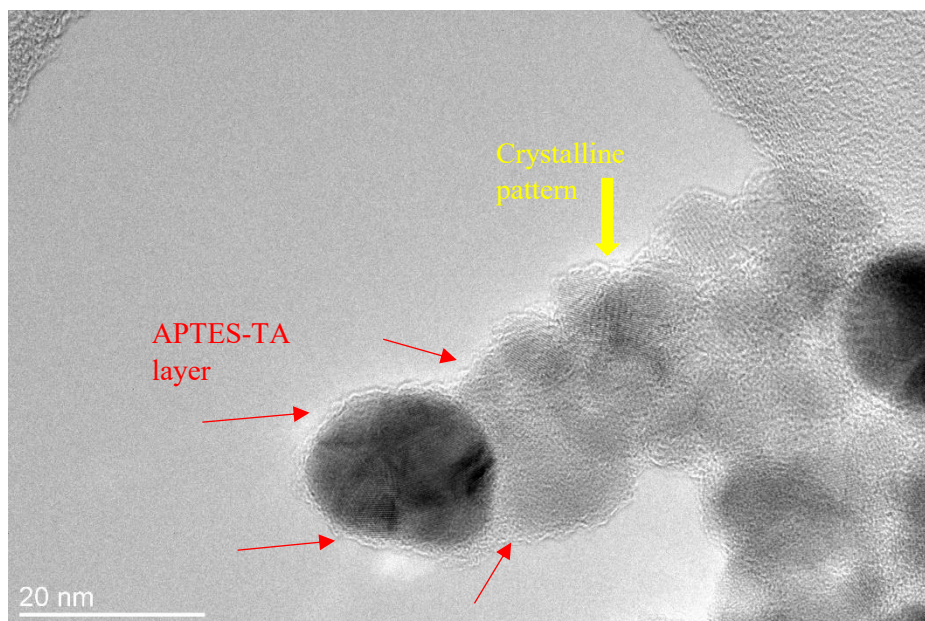


FIGURE 5.3 TEM ANALYSIS OF MAGNETITE NANOPARTICLES (AC+APTES) AND SILVER NANOPARTICLES REDUCED VIA TA

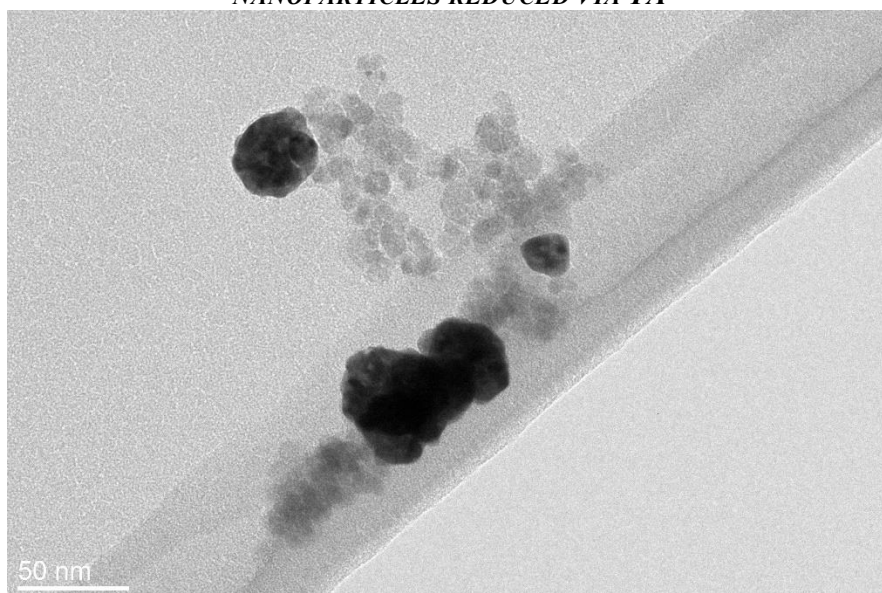


FIGURE 5.4 TEM ANALYSIS OF MAGNETITE NANOPARTICLES (AC+APTES) AND GOLD NANOPARTICLES REDUCED VIA TA

In figure 5.2, as well as in figure 5.3, can be noticed the thin layer of organic surfactants (mostly tannic acid and APTES) that surrounds the nanocomposites, proving the success of the coating process for both samples, the one with functionalized with silver and the one with gold.

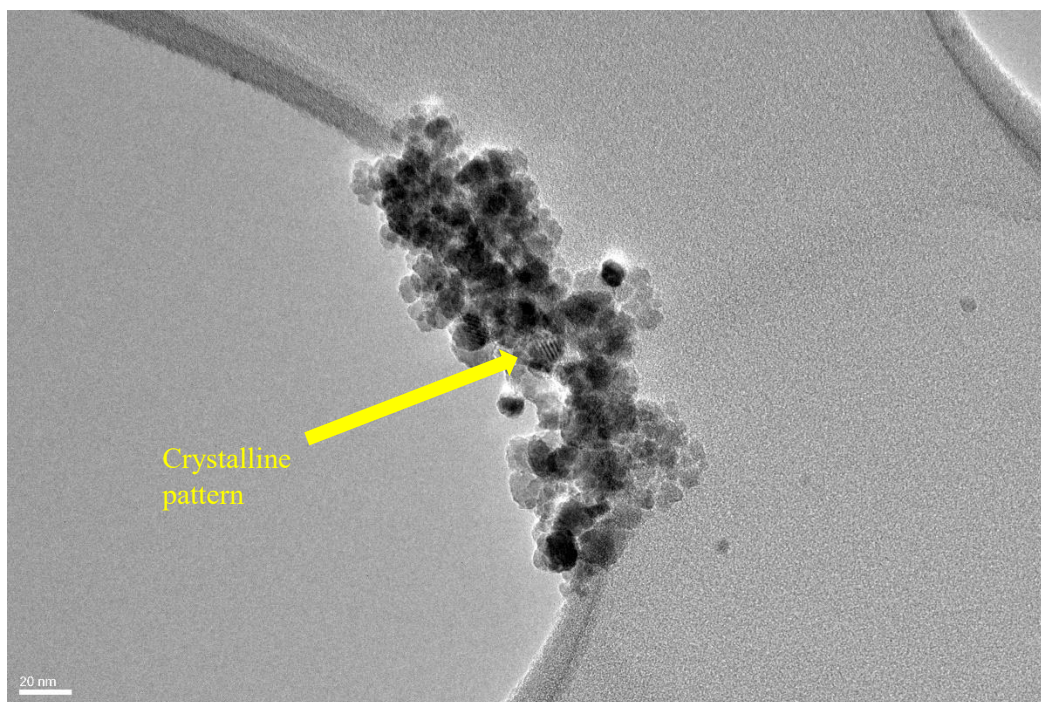


FIGURE 5.5 TEM ANALYSIS OF PURE MAGNETITE NANOPARTICLES

Again, in figure 5.3 and 5.5, it is shown, talking about magnetite nanoparticles, the typical pattern of crystalline structures.

STEM analyses were also performed to investigate all areas in which iron and gold/silver were detected and to get a general view of the sample, in order to understand its morphology and distribution of the metal nanoparticles. In figure 5.6 and 5.7, the bright spots are respectively gold and silver nanoparticles reduced onto the magnetite surface with tannic acid. To be noticed, the resolution of this technique is limited, hence cannot be used to determine the structure of the nanocomposites, but it is useful to determine the distribution of noble metals nanoparticles in the sample.

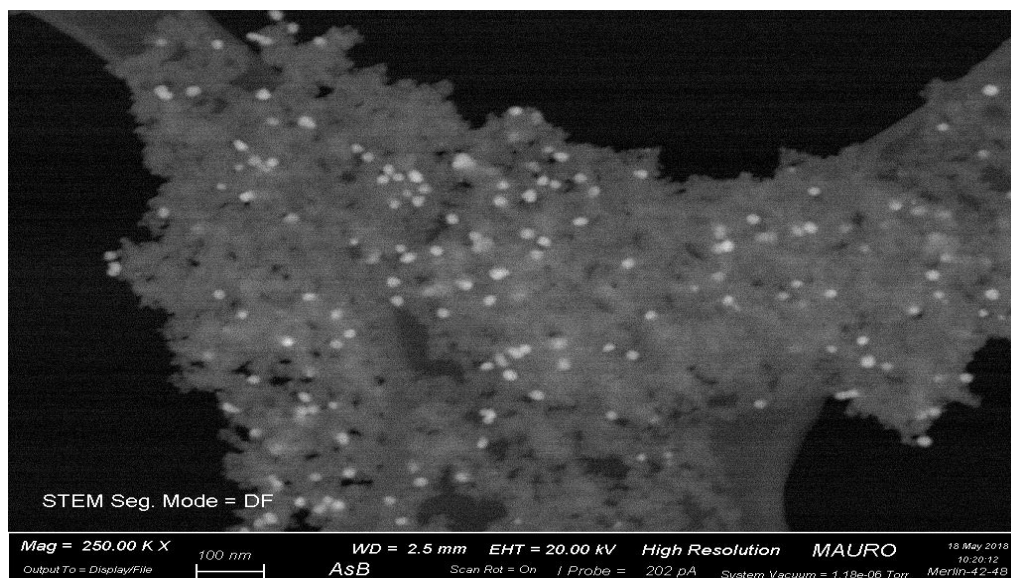


FIGURE 5.6 STEM ANALYSIS OF IRON OXIDE NANOPARTICLES FUNCTIONALIZED WITH AC+APTES AND GOLD NANOPARTICLES

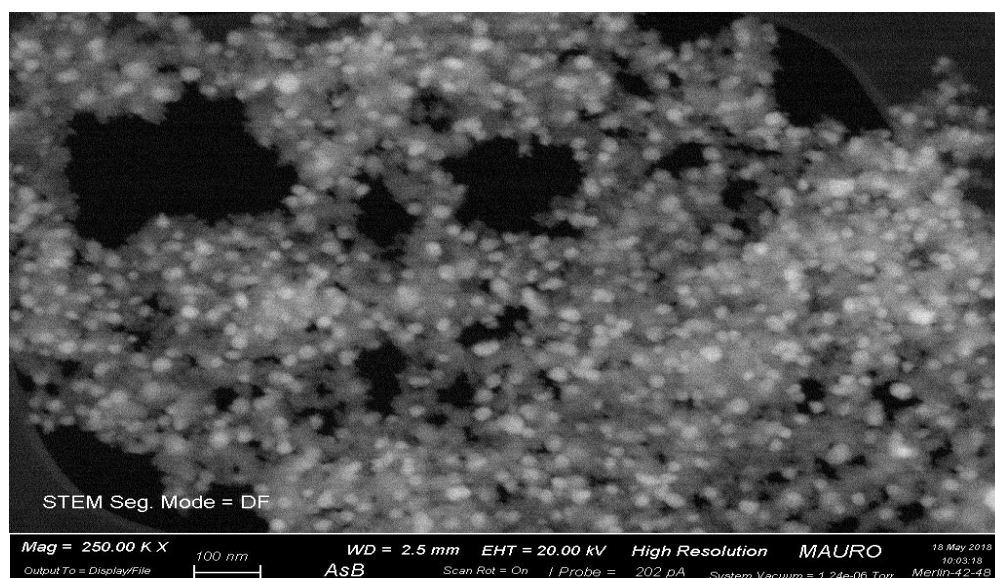


FIGURE 5.7 STEM ANALYSIS OF IRON OXIDE NANOPARTICLES FUNCTIONALIZED WITH AC+APTES AND SILVER NANOPARTICLES

As can be seen in the previous images, however, Au and Ag were located on the magnetite surface. Both synthesis methods are characterized by uniform growth of metal nanoparticles, especially the one with silver nanoparticles; the reduction of gold salt produced few gold nanoparticles because of its low quantity at the beginning. The range of the diameter dimension is determined directly from the software, in general, approximately [20-40] nm.

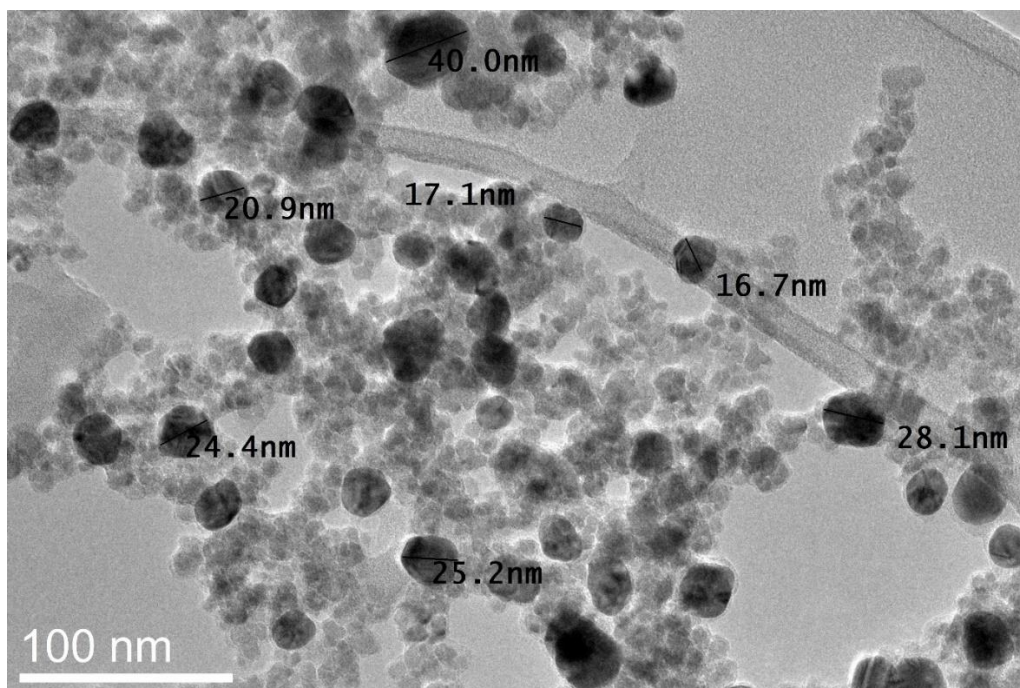


FIGURE 5.8 TEM IMAGE OF MAGNETITE FUNCTIONALIZED WITH APTES AND SILVER NANOPARTICLES

However, the aim of this work was to find an easy way to reduce gold and silver nanoparticles onto magnetite surface using tannic acid. Therefore, this first synthesis route provides good results, especially regarding the magnetite and silver one.

5.1.2 Second synthesis route

The achievement of a suitable surface functionalization of the particles and the choice of the correct amount of chemical reagents involved in the process are crucial to obtain good results in terms of stability and aggressive power of the nanoparticles. As said in the previous chapter, tannic acid, being able to hydrolyze into gallic acid and glucose and to form quinone groups, is characterized by an aggressive reducing power and can grant good stabilization under alkaline conditions. For these reasons, TA was used as stabilizing and reducing agent because of its well-known good effect (32,N+TA,reviewing the tannic acid). [46],[48],

To further investigate the surface of tannic acid coated Fe_3O_4 nanoparticles, the FT-IR spectra were detected. In figure 5.9, the main band at 3450 cm^{-1} is due to the OH groups, indicating the presence of polyphenols in the material; furthermore, peaks deriving from the presence of $\text{C}=\text{O}$ ($\sim 1740\text{ cm}^{-1}$), as well as $\text{C}=\text{C}$ (aromatic stretching, 1630 cm^{-1}) and $\text{C}-\text{O}(\text{H})$ (sugar moiety stretching, 1088 cm^{-1}) are detected. Based on these results, is rightful to suggest that iron oxide nanoparticles were successfully coated with tannic acid compound.

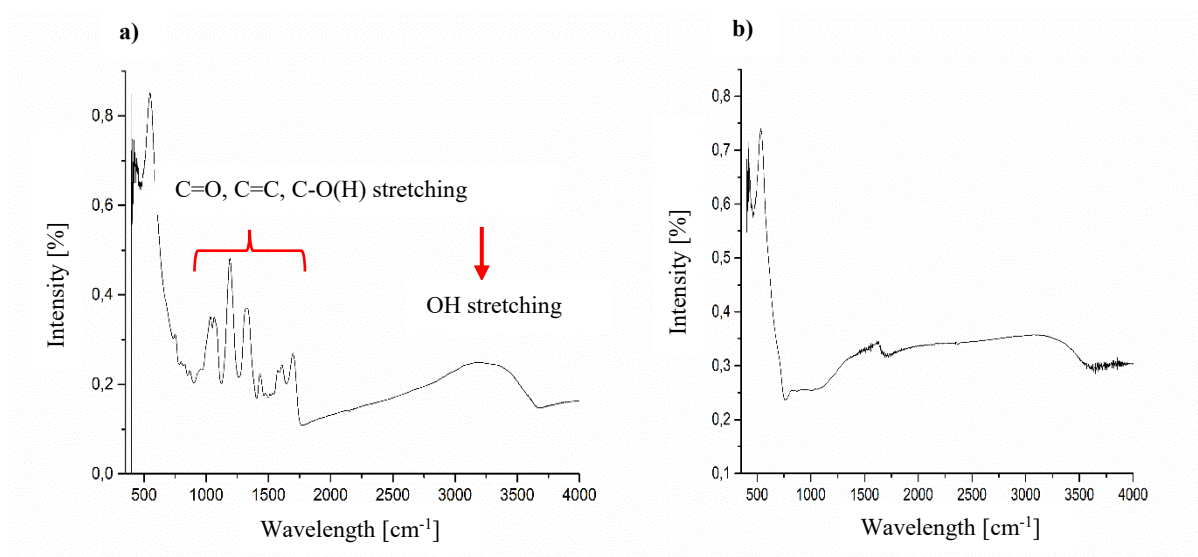


FIGURE 5.9 FT-IR OF A) MAGNETITE AND TANNIC ACID AND B) PURE MAGNETITE NANOPARTICLES

Tannic acid as stabilizing and reducing agent has been successfully adopted, involving seeding of silver nanoparticles on iron oxide substrates to form nanocomposites as shown in figure 5.10 and 5.11.

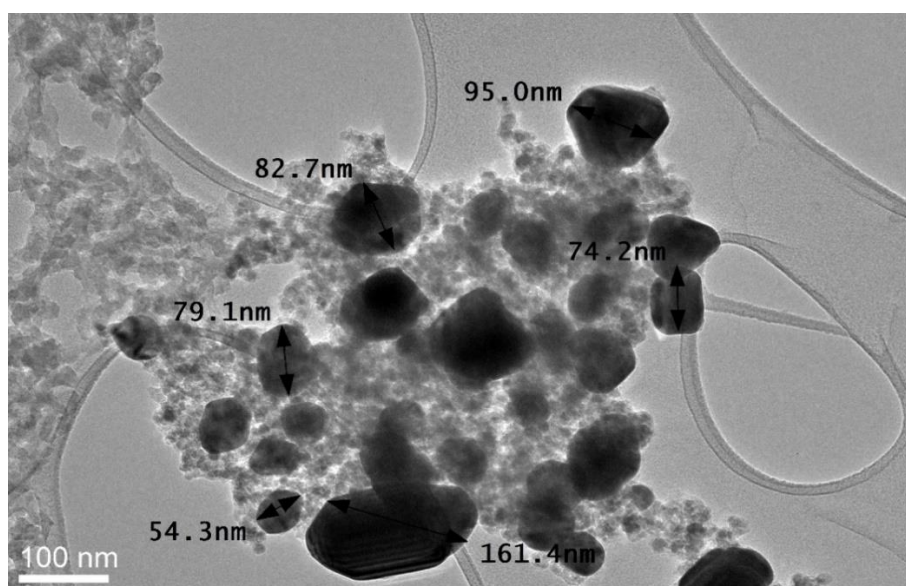


FIGURE 5.10 TEM IMAGE OF MAGNETITE AND SILVER NANOCOMPOSITE. TANNIC ACID USED AS STABILIZING AND REDUCING AGENT

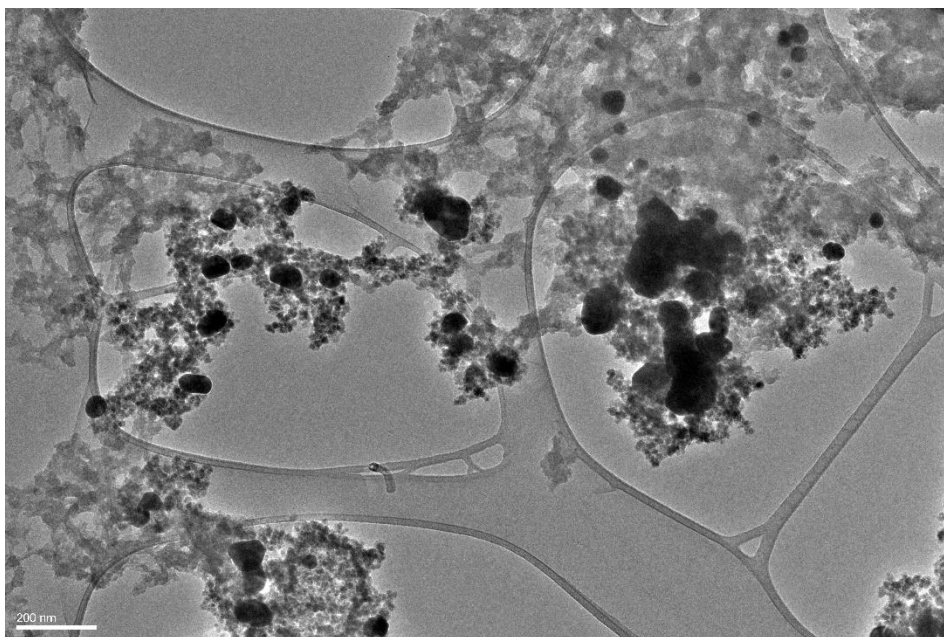


FIGURE 4.11 TEM IMAGE OF MAGNETITE AND SILVER NANOCOMPOSITE. TANNIC ACID USED AS STABILIZING AND REDUCING AGENT

As can be seen, the silver nanoparticles embedded into the iron oxide mass are still not optimal to be considered, overall, nanocomposites. Hence, optimizations are to be taken through, especially regarding correct amount of chemical salts and ratio between TA and AgNO_3 . Nevertheless, it is clear that the silver particles, with a dimension range of [70-160] nm, are attached onto the magnetite fine nanoparticles, thanks to the washing procedure adopted.

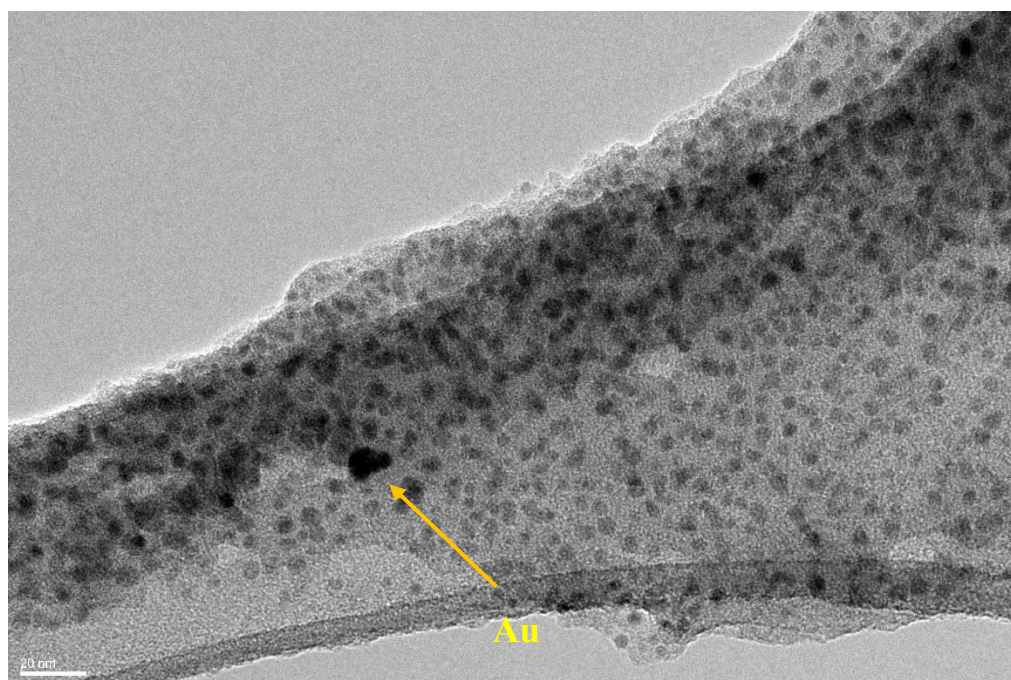


FIGURE 5.12 TEM IMAGE OF IRON OXIDE-GOLD NANOCOMPOSITE. TA AS REDUCING AND STABILIZING AGENT

Different results came from the analysis of the iron oxide-gold nanocomposites: once again, the strong stabilizing ability of the tannic acid has been confirmed, as it can be seen in Figure 5.12 (fine magnetite nanoparticles dispersed in the organic matrix of TA), but further optimization must be conducted to find the correct synthesis routes and have a major quantity of gold nanoparticles onto magnetite's surfaces.

These results have been further confirmed by EDS analyses. Figure 5.13 shows that Au nanoparticles, with a characteristic peak at 2.120 KeV, were not detected, probably because too small and not enough in quantity. Cu, C from the grid and Fe where, on the contrary, easily detected even after 1 min of exposition (max exposition time= 2 minutes).

Different situation with the results coming from EDS analysis of magnetite and silver nanocomposites (Figure 5.14): silver has been detected in a good amount. Again, Cu and C from the grid and Fe and O, proving the presence of iron oxide compound, were detected as well.

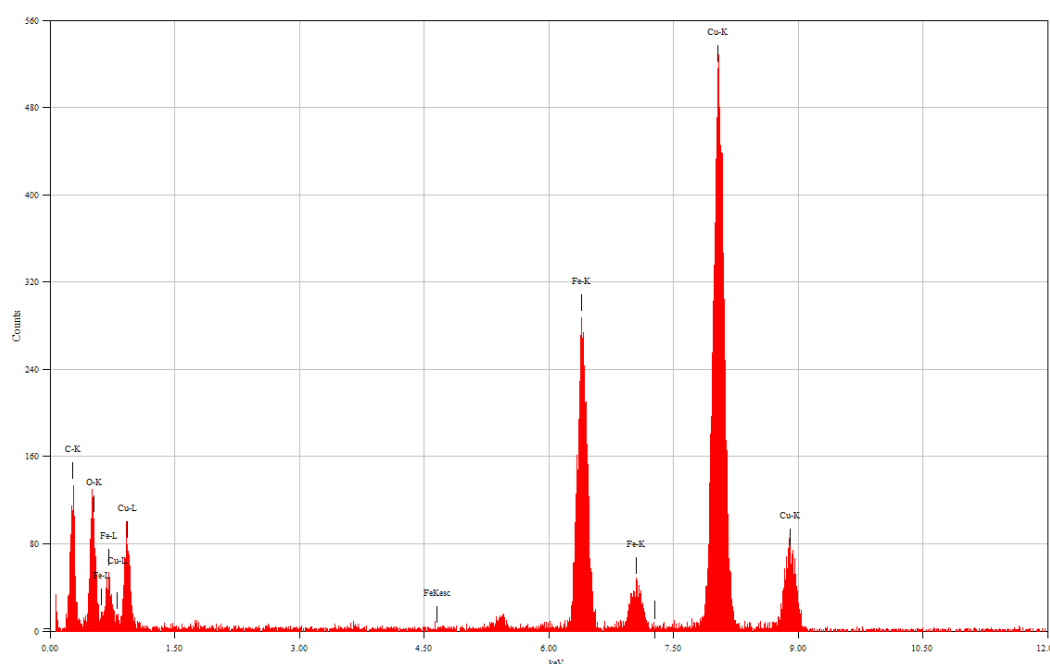


FIGURE 5.13 EDS ANALYSIS OF MAGNETITE-GOLD NANOCOMPOSITES. TA AS REDUCING AND STABILIZING AGENT

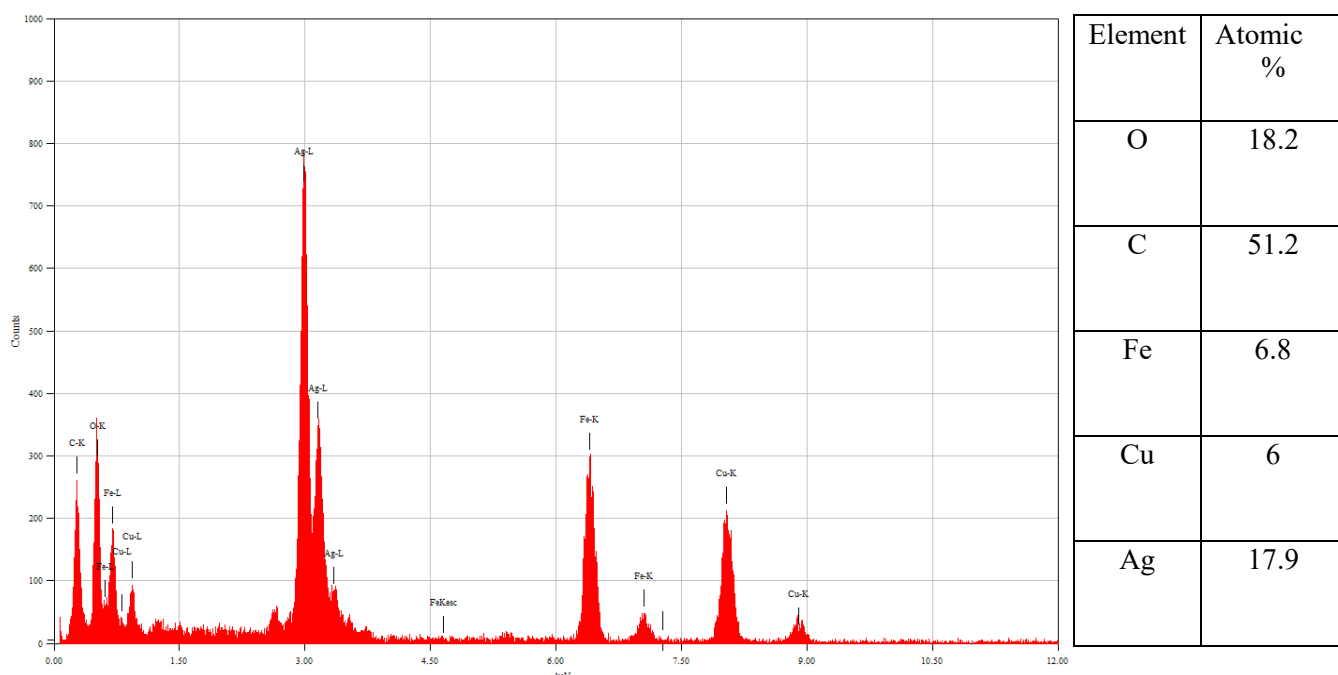


FIGURE 5.14 EDS ANALYSIS OF MAGNETITE-SILVER NANOCOMPOSITES. TA AS REDUCING AND STABILIZING AGENT

Finally, it is worth to mention the results from the SAED: all the images are characterized by the pattern of each sample on which are overlapped the simulated SAED pattern of Fe_3O_4 , gold and silver.

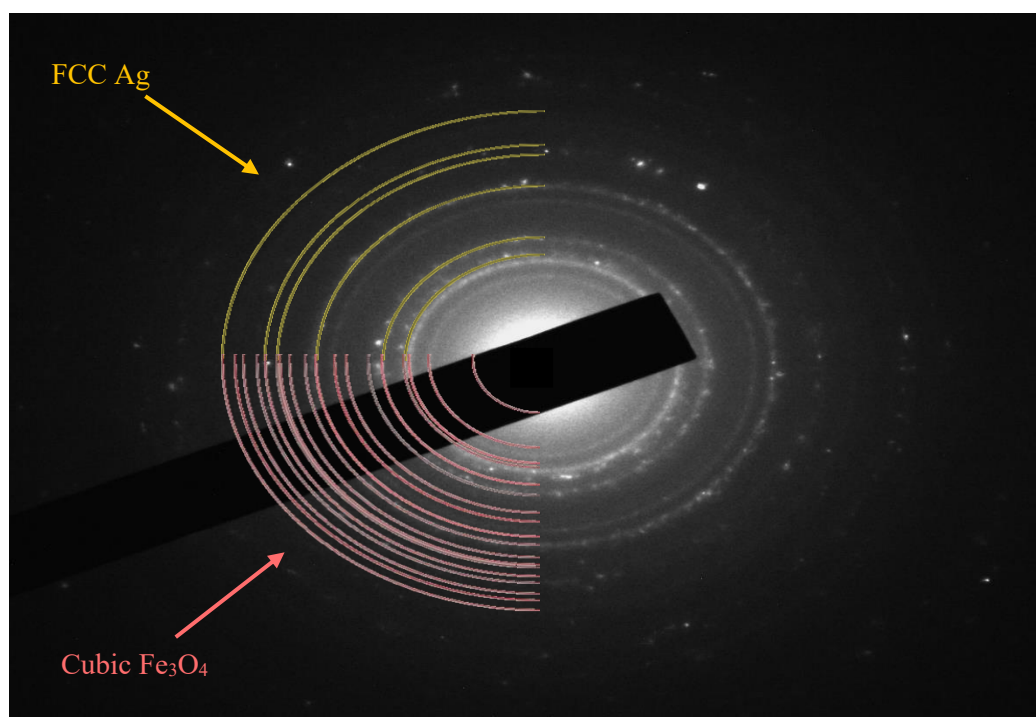


FIGURE 5.15 SAED RESULTS OF MAGNETITE FUNCTIONALIZED WITH SILVER, OVERLAPPED BY SIMULATIONS: RED FOR MAGNETITE AND YELLOW FOR SILVER

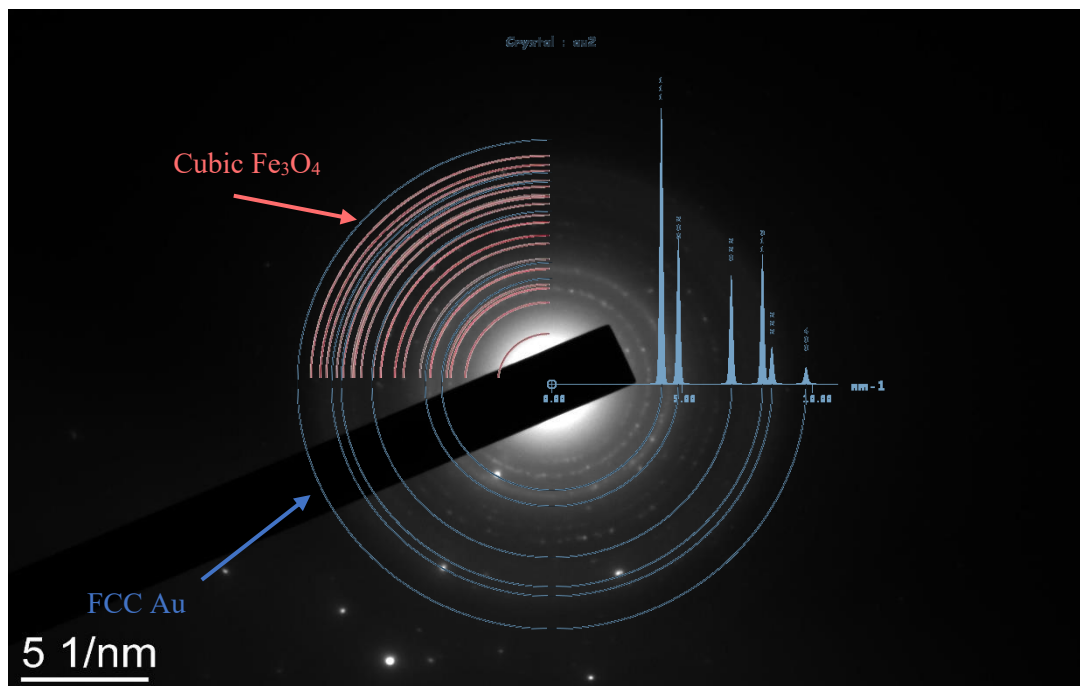


FIGURE 5.16 SAED RESULTS OF MAGNETITE FUNCTIONALIZED WITH GOLD OVERLAPPED BY SIMULATIONS: RED FOR MAGNETITE AND BLUE FOR GOLD

It can be seen how the simulations match the results, especially in the case of magnetite and silver (figure 5.15); as for concerns the sample magnetite and gold (figure 5.16), the majority is characterized by Fe_3O_4 , while gold can be represented by a couple of bright spots, indicating its low concentration. Next, to testify the possibility of these nanocomposites to work as a bifunctional material, the magnetic, optical and hemotoxicological properties are estimated.

5.2 Magnetic properties

To manage these nanocomposites using a magnetic field is one of the main reasons for utilizing Fe_3O_4 particles as support for noble metal nanoparticles. Hence, it is vital to determine the effect that Au/Ag nanoparticles have on the magnetic properties of pure magnetite nanoparticles. As indicated in figure 5.17, iron oxide NPs show higher magnetization in comparison with the other samples, due to its lack of any external coating that lower these properties. In addition, all 4 functionalized samples show no hysteresis, no remanence or coercivity, which is in agreement with superparamagnetic behavior of magnetite. Nevertheless, the decrease in the saturation magnetizations is linkable with the diamagnetic nature of silver and gold, yet the

value of these magnetization was still enough to apply magnetic separation for washing procedures, as stated in the previous chapter.

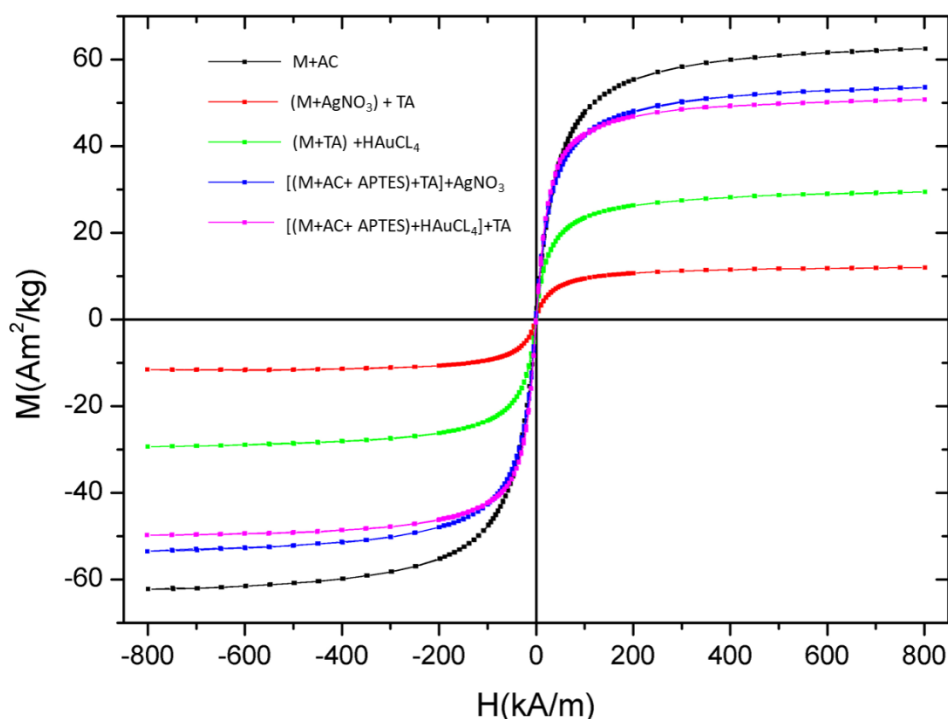


FIGURE 5.17 *VSM ANALYSIS OF PURE IRON OXIDE AND IRON OXIDE - GOLD/SILVER NANOCOMPOSITES*

Superparamagnetic behavior is shown by all the samples and it is correlated with the dimension of the magnetic nanoparticles, that should be below the Superparamagnetic size limit (SPL), which is, for the magnetite (Fe_3O_4), $\text{SPL}=24$ nm.

The decrease in magnetization is, hence, mainly ascribable to the presence of gold and silver nanoparticles on the surface of the magnetite, a consequence that is not possible to avoid. The main difference notable is between the nanoparticles functionalized with citric acid and APTES and those with only tannic acid: this is probably because of the major amount of tannic acid, when used as stabilizing agent too, causing a thick coating around the magnetite nanoparticles, which aggressively shields their magnetic response.

Despite this, it is proven clear that the grafting of the metal particles does not influence excessively the magnetic properties of the precursor magnetite nanoparticles, so they could be easily separated using a magnet, granting the complete attachment onto the magnetite surface.

5.3 Optical properties

Before talking about the optical properties results, it is important to underline the fact that before committing them, as well as the hemotoxicological tests, ICP-MS results were accomplished to acquire the correct concentration to use for each sample.

TABLE 5.1 ICP-MS RESULTS

Sample No.	Sample name	Fe (mg/mL) expected	Fe (mg/mL) measured	Au (mg/mL) expected	Au (mg/mL) measured	Ag (mg/mL) expected	Ag (mg/mL) measured	Total (mg/ml)
1	M+AC	4	6.01 ± 0.30	/	/	/	/	6.01
2	M+TA+Au	2	2.38 ± 0.01	0.01	0.005 ± 0.001	/	/	2.385
3	M+AC+APTES+Au	1	0.138 ± 0.004	0.01	0.018 ± 0.001	/	/	0.156
4	M+TA+Ag	15	3.25 ± 0.12	/	/	0.5	6.56 ± 0.06	9.81
5	M+AC+APTES+Ag	0.15	0.072 ± 0.001	/	/	0.05	0.053 ± 0.002	0.125

According to these results, all the samples were normalized to two concentrations, starting from the lowest among them (the concentration of M+AC+APTES+Ag), to continue with their characterization: $c_1 = 0.1$ mg/ml and $c_2 = 0.035$ mg/ml.

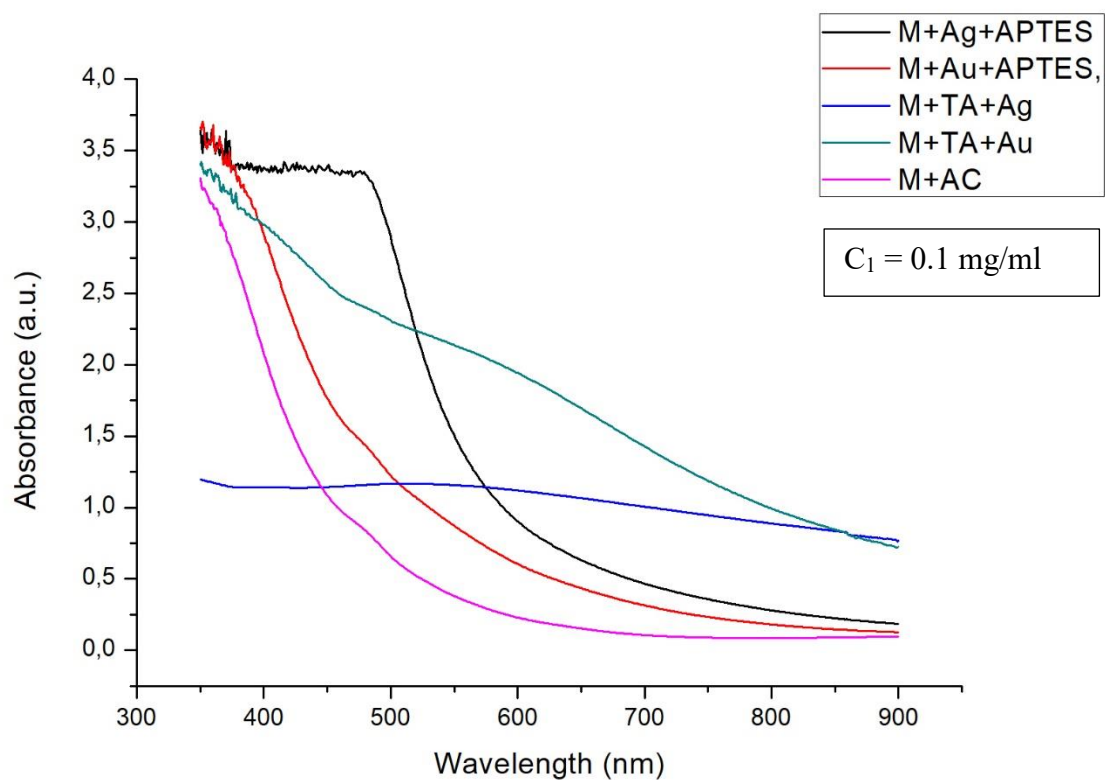


FIGURE 5.18 UV-VIS ABSORPTION SPECTRA OF NANOCOMPOSITES. SAMPLES' CONCENTRATION $C_1 = 0.1 \text{ MG/ML}$

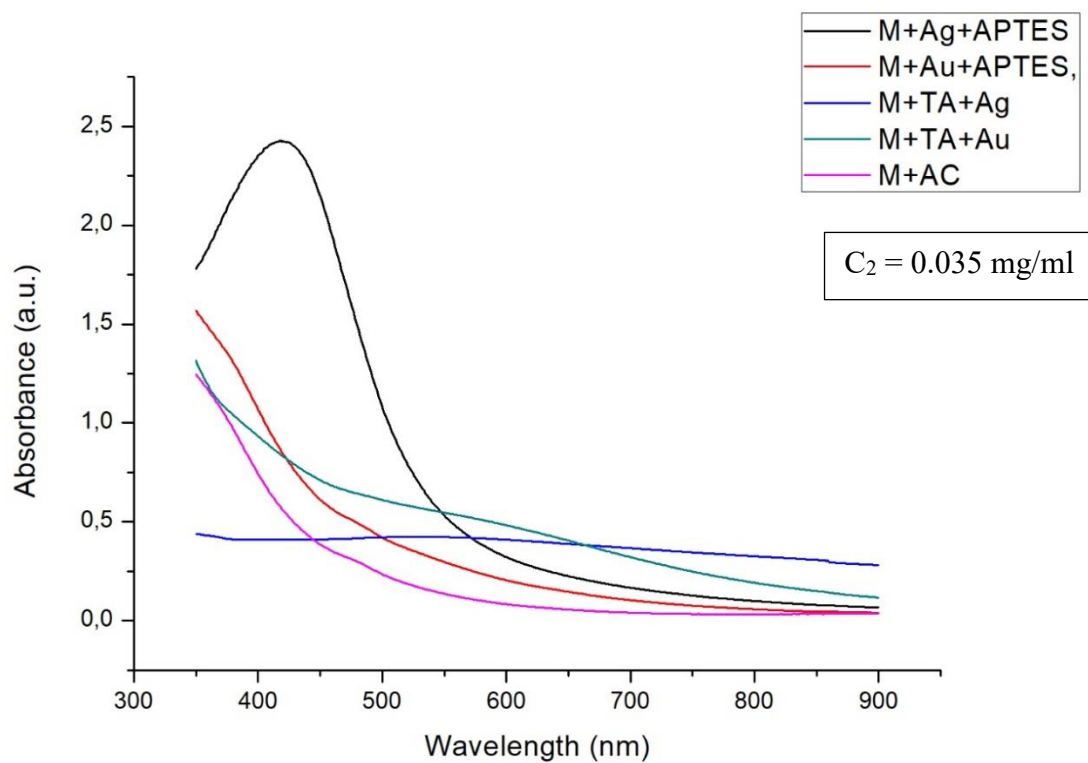


FIGURE 5.19 UV-VIS ABSORPTION SPECTRA OF NANOCOMPOSITES. SAMPLES' CONCENTRATION $C_2 = 0.035 \text{ MG/ML}$

As it becomes obvious from the start, concentration of the samples is one of the ruling parameters. All the solutions are dispersed in water.

In figure 5.18, regarding concentration c_1 , the two samples functionalized with APTES are still too concentrated to be analyzed, as it results clear from the noise that characterizes short wavelengths. A completely different situation characterizes samples with concentrations c_2 (figure 5.19), where, for example taking in exam sample M+APTES+Ag, it is depicted by a smooth peak centered in the characteristic range of silver SPR. Nevertheless, for both concentrations, the samples functionalized only with tannic acid delineate differences in absorption peaks: as, for example, for M+TA+Ag, where the presence of a considerable amount of large silver nanoparticles and thick organic coating layer causes a weakening in absorption spectra common to the rest of the solutions.

5.3.1 Thermal experiments

In figures 5.20 and 5.21, it is possible to observe the heating rates of the samples, normalized at the concentrations c_1 and c_2 , after being irradiated for 10 minutes with a laser power of 1 W. The temperatures have been acquired with a time step of 1 minute.

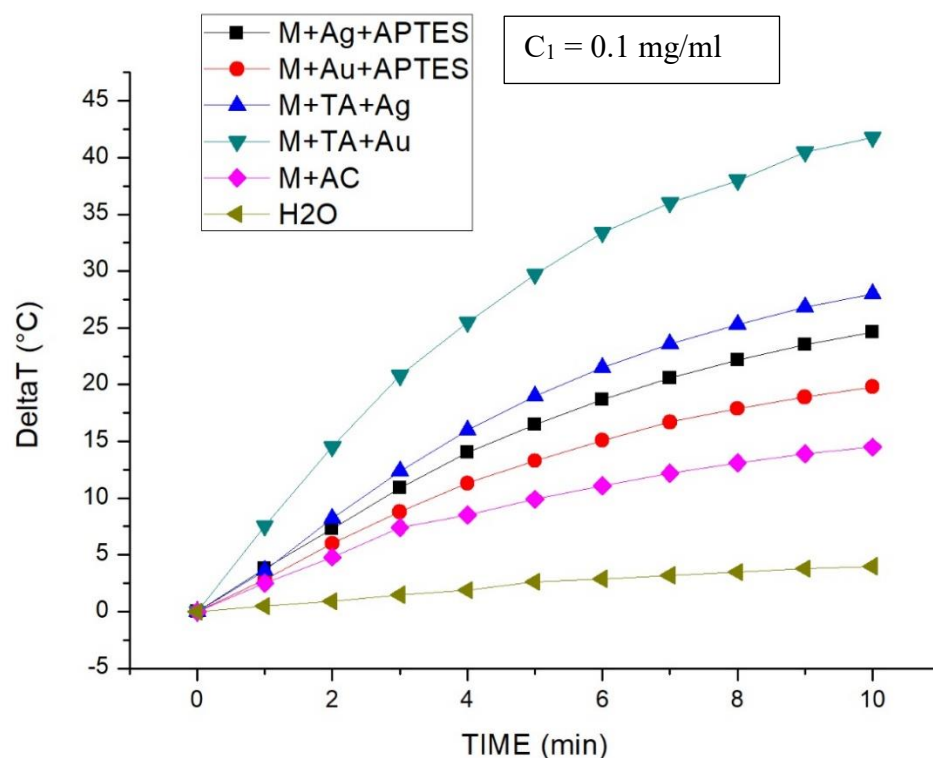


FIGURE 5.20 **PHOTOTHERMAL RESULTS OF ALL NANOCOMPOSITES. CONCENTRATION $C_1=0.1$ MG/ML**

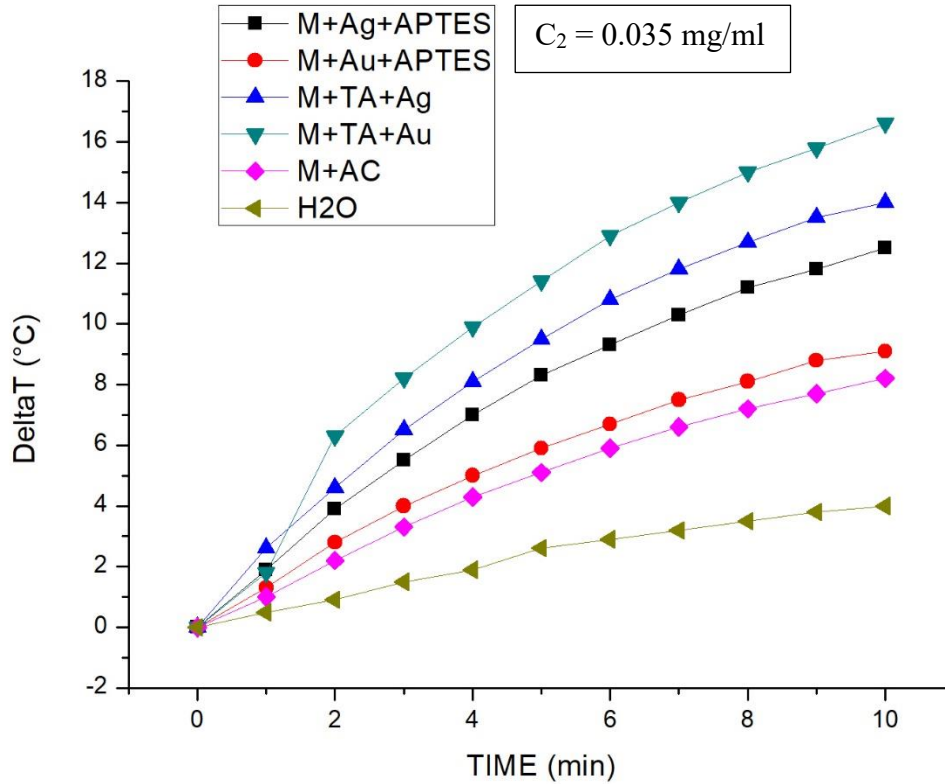


FIGURE 5.21 PHOTOTHERMAL RESULTS OF ALL NANOCOMPOSITES. CONCENTRATION $C_2 = 0.035$ MG/ML

After the evaluation of these results coming from the photothermal tests, it is clear that, between the two concentrations taken in exam, only with $C_2 = 0.035$ mg/ml the average temperatures are not excessive and near a certain compatibility with a biological application.

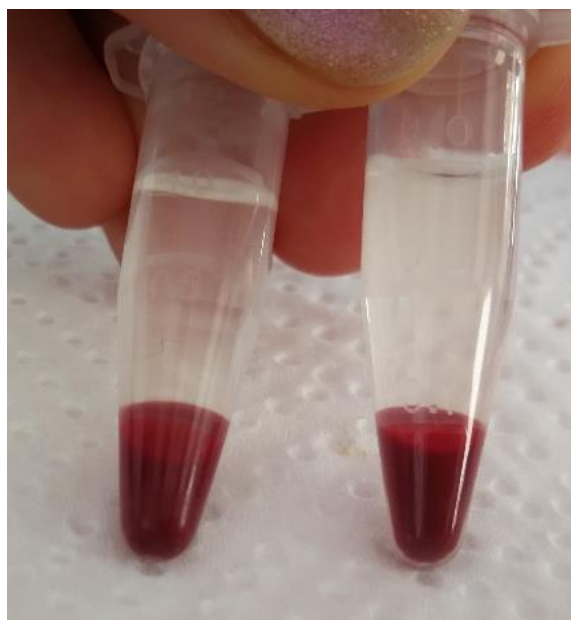
Anyway, in general, all the results are coherent as expected: the presence of noble metal nanoparticles, giving SPR properties to pure magnetite nanoparticles, granted higher heating rate to the nanocomposites; the heating rate is directly dependent on the concentration of the metal components. In particular, the sample M+TA+Au is characterized by the highest heating rate among all the solutions: this can be attributed to higher absorption spectra at the characteristic wavelength of the irradiation. Finally, to be noticed that in both cases it is possible to observe that the heating rate is higher for the nanocomposites without APTES: this can be due to the absence of its layer, which could decrease the photothermal effect.

5.4 Hemotoxicological properties

Talking about hemotoxicological properties, this test was performed in order to evaluate the toxicological effect of the nanocomposites in contact with red blood cells (RBCs).

These cells were isolated from the fresh whole sheep blood supplied by Veterinary Faculty (University of Ljubljana, Slovenia) in Alsever's medium (TCS Biosciences Ltd, UK) and used within two days. Before use, RBCs were washed with physiological 0.9% NaCl solution, centrifuged (at 600 rpm for 15 min) and then the supernatant was discarded. Two more NaCl washes were performed before use.

a)



b)

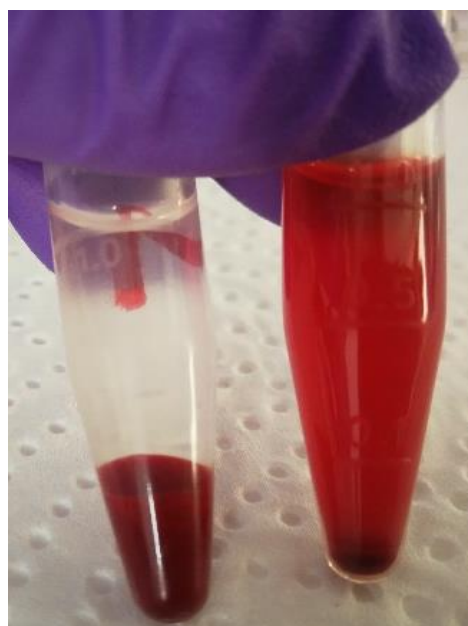


FIGURE 5.22 A) RED BLOOD CELLS AFTER PERFORMING 3 NaCl WASHES. B) SUPERNATANT REPLACED WITH HBS (LEFT) AND DISTILLED WATER (RIGHT). THE LATTER WILL BE TAKEN AS POSITIVE CONTROL.

Hemolysis of RBCs was evaluated before and after incubation with nanoparticles by measuring hemoglobin absorbance at 541 nm using a spectrophotometer (BioTek Synergy H4 Hybrid microplate reader). It was found that, before incubation, hemolysis was negligible (0.3 %).

RBCs were resuspended in sterile HBS buffer with 0.9 wt% NaCl to obtain 5 vol.% cell density.

TABLE 5.2 ICP-MS RESULTS

Sample No.	Sample name	Fe (mg/mL) measured	Au (mg/mL) measured	Ag (mg/mL) measured	Total (mg/mL)
1	M+TA	6.01 ± 0.30	/	/	6.01
2	M+TA+Au	2.38 ± 0.01	0.005 ± 0.001	/	2.385
3	M+TA+Au+APTES	0.138 ± 0.004	0.018 ± 0.001	/	0.156
4	M+Ag+Au	3.25 ± 0.12	/	6.56 ± 0.06	9.81
5	M+TA+Ag+APTES	0.072 ± 0.001	/	0.053 ± 0.002	0.125

Concentration of NPs for all samples was 35 or 100 $\mu\text{g/mL}$ (total metal concentration determined via ICP-MS analysis). Total volume in each vial was 200 μL , which will be 100 μL of 10% RBCs + 100 μL of NPs; this is true for samples 1,2 and 4 as shown in table 5.2, while for the other two samples 3 and 5 (table 5.2), modifications are needed because their concentrations are too low. All samples were measured in triplicates.

TABLE 5.3 CONCENTRATIONS OF THE SAMPLES USED DURING THE TESTS

SOLUTION	200µg/ml	70µg/ml	NaCl	RBC (10 %)
Sample 1: M+AC	96 µg	96 µg	4 µg	100 µl
Sample 2: Ag+TA	96 µg	96 µg	4 µg	100 µl
Sample 4: Au+TA	96 µg	96 µg	4 µg	100 µl

SOLUTION	Initial solution	NaCl	RBC
Sample 5: Ag+APTES, 100 µg/ml	154 µl	6 µl	40 µl (25 wt%)
Sample 3: Au+APTES, 100 µg/ml	123 µl	5 µl	72 µl (14 wt%)
Sample 5: Ag+APTES, 35 µg/ml	54 µl	2 µl	144 µl (7 wt%)
Sample 3: Au+APTES, 35 µg/ml	43 µl	2 µl	155 µl (6,5 wt%)

The number of cells that lysed after incubation at 37°C for 5h was evaluated by centrifuging samples and measuring the hemoglobin absorbance of the supernatant. The Absorbance intensity, corresponding to the 100% lysed cells (I_{100}), was evaluated by lysing control samples with deionized water via hypotonic osmotic shock and measuring hemoglobin absorbance. Percent hemolysis was then calculated as follows:

$$\text{hemolysis (\%)} = 100 \cdot \frac{I_{\text{sample}}}{I_{100}} \quad (1)$$

where I_{sample} represents the absorbance intensity of lysed cells obtained during incubation with NPs or control samples (no NPs).

TABLE 5.4 HEMOTOXICITY RESULTS

Sample (µg/ml)	Hemolysis (%)
1 (35)	1.9
1 (100)	1.8
2 (35)	5.5
2 (100)	3.7
3 (35)	1.9
3 (100)	2.1
4 (35)	3.9
4 (100)	2.6
5 (35)	2.3
5 (100)	5.4
Negative Control	2.8
HBS Buffer	0
Positive Control	100

From hemotoxicity results (table 5.4), it is possible to notice that after one day of incubation, the nanoparticles showed minimal hemotoxicity, comparable to that of the negative control sample. In fact, for each sample of RBC is founded that the hemolysis is very low (lower than 5.4% for all the samples), this means that the NPs toxicity at these concentrations is negligible and therefore they are potentially usable for clinic application.

6. Conclusions and future developments

The aim of this project was to optimize a simple approach to immobilize silver and gold nanoparticles onto chemically modified surface of magnetite nanoparticles, in order to obtain well dispersed iron oxide – gold/silver nanocomposites in aqueous media, using tannic acid as reducing or reducing and stabilizing agent. The combination of hyperthermia for iron oxide nanoparticles (magnetic-induced hyperthermia) and Ag/Au (photo-induced hyperthermia) nanoparticles has the advantage of making these nanocomposites appropriate candidates to generate a cytotoxic environment and enable cancer theranostic.

The iron oxide – metal nanocomposites have been characterized to improve knowledge of magnetic and plasmonic nanoparticles used in biomedical applications.

The main results that came out from experimental data are:

- According to previous thesis works, magnetite nanoparticles with spherical shape and a dimensional range of few nanometers can be successfully synthesized with co-precipitation method.
- According to the literature and to previous works, a stable suspension was obtained thanks to citric acid in a highly basic environment (pH was adjusted to 10 in order to avoid agglomeration in further synthesis steps).
- The utility of APTES as a connection for the attachment of metal nanoparticles onto previously dispersed iron oxide nanoparticles by citric acid has been confirmed.
- Tannic acid resulted in an interesting solution as reducing agent, but it can not guarantee the same good results of citric acid as stabilizing agent.
- VSM, UV-vis and laser analyses testified that the nanocomposites maintain the optical properties of metal nanoparticles and the magnetic characteristics of iron oxide nanoparticles.
- Hemotoxicological tests, in the end, proved that the samples are not dangerous for healthy blood cells.

Future developments can consider improving the application of tannic acid also as stabilizing agent and improve its purpose as reducing agent, starting, for example, from the tuning of the pH value during the seeding process of the metal nanoparticles.

Here follows an early attempt of optimization, according to what it is stated above:

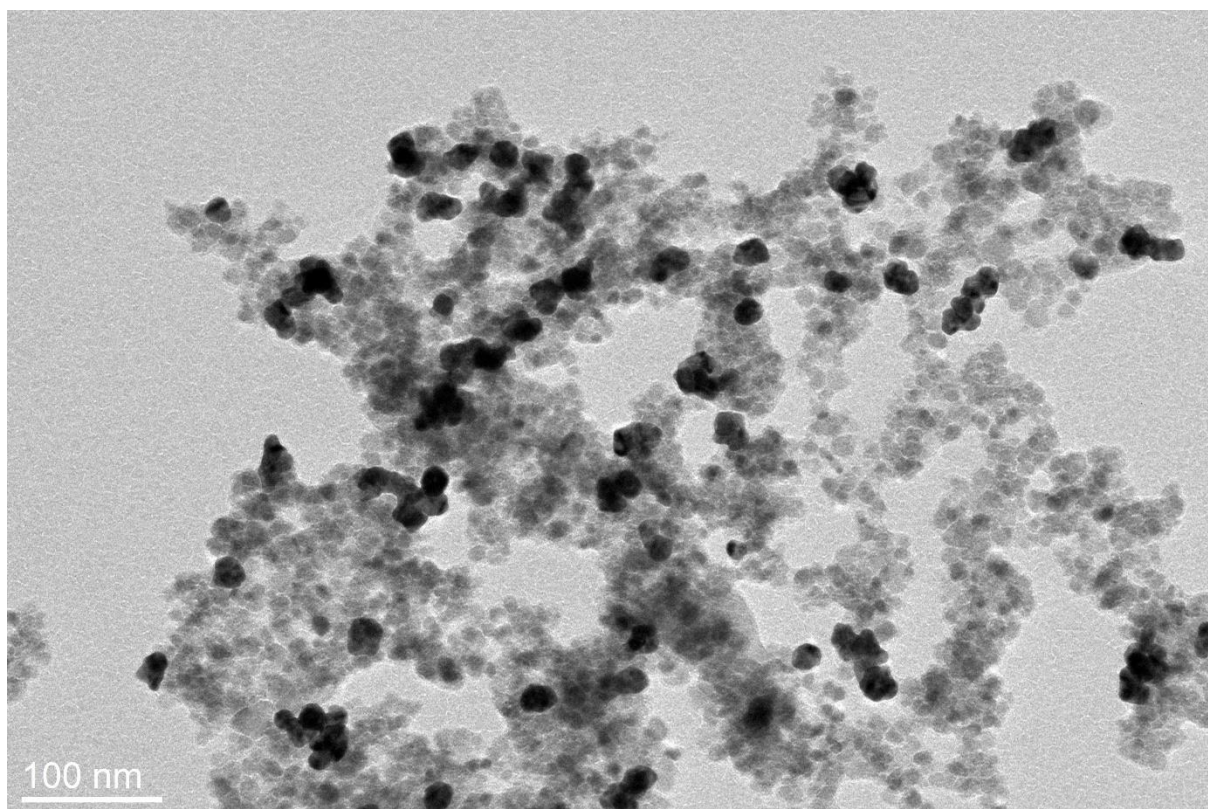


FIGURE 6.1 OPTIMIZED SOLUTION MAGNETITE+APTES+AU

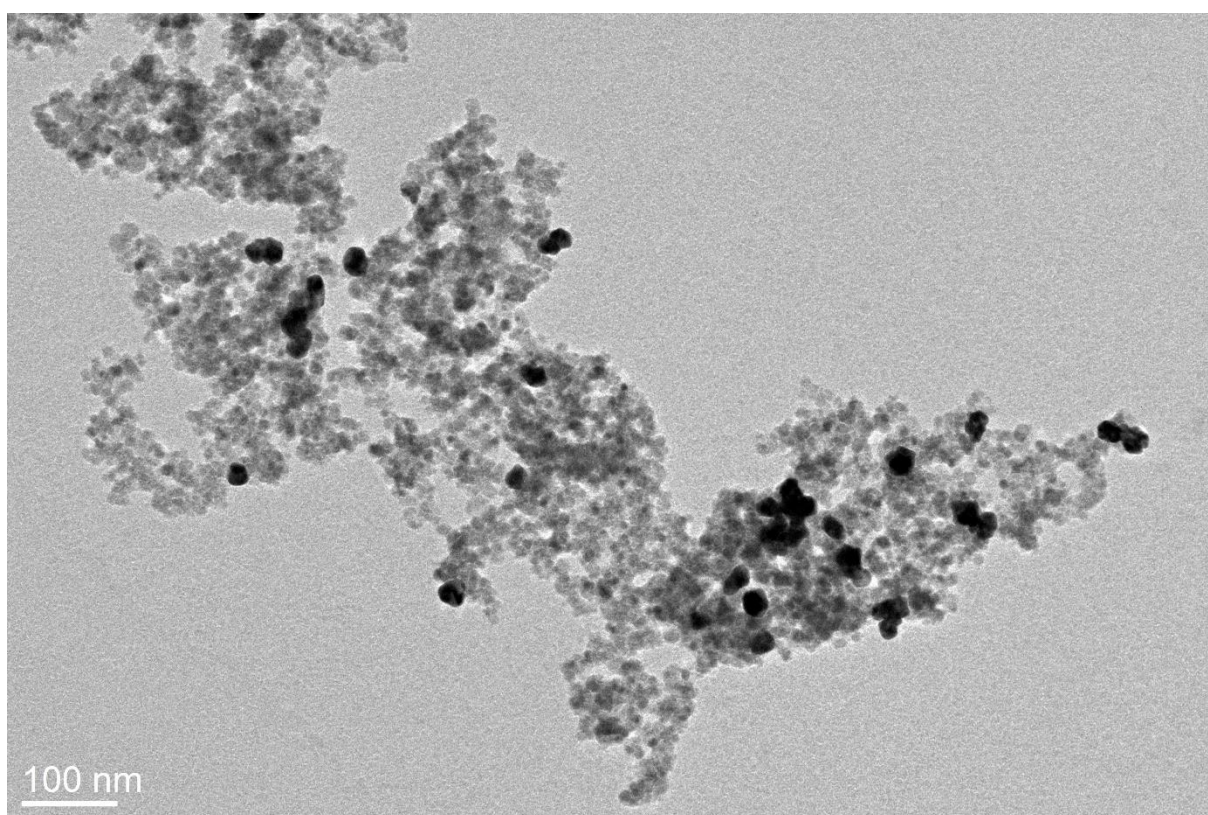


FIGURE 6.2 OPTIMIZED SOLUTION MAGNETITE+APTES+AU

As it results from figure 6.1 and 6.2, the increased amount of gold nanoparticles testified the good achieving of the optimization intents: in this case, the “first route synthesis”, involving magnetite, citric acid, APTES and gold was repeated, but, before adding gold to the solution, its pH was adjusted to a mild-basic value (pH=7).

The contribution of the optimization of the synthesis process is that offers not only a nanocomposite system with controlled magnetic and plasmonic features but also a valid and rapid alternative synthesis route to the existing ones, characterized by only one eco-friendly and non-toxic chemical agent, namely the tannic acid.

Acronyms

AC	Alternate current
APTES	(3-aminopropyl) triethoxysilane
CA	Citric acid
DLVO	Derjaguin, Landau, Verwey and Overbeek
EDS	Energy dispersive X-ray spectroscopy
EPR	Enhanced permeation and retention
HEPA	High efficiency particulate air filter
ION	Iron oxide nanoparticles
M	Magnetite
MDR	Multi-drug resistance
MRI	Magnetic resonance imaging
MRP	Multi-drug resistance associated protein
NP	Nanoparticles
PEG	Polyethylene glycol
PLA	Poly(lactide acid)
PVA	Poly(vinyl alcohol)
RES	Reticuloendothelial system
ROS	Reactive oxygen species
SAR	Specific absorption rate
SLP	Specific loss power
SPION	Superparamagnetic iron oxide nanoparticles
SPR	Surface plasmon resonance
STEM	Scanning transmission electron microscopy

Symbols and constants

Symbol	Definition	Unit of measure
M	Intensity of magnetization	[A/m]
H	Magnetic field	[A/m]
B	Magnetic induction	[A/m]
k	Magnetic susceptibility in terms of volume	Dimensionless
χ	Magnetic susceptibility in terms of mass	Dimensionless
μ	Magnetic permeability	[H/m]
T	Temperature	°C or K
V	Volume	[m ³]
S	Surface	[m ²]
τ	Characteristic relaxing time	[s]
KV	Anisotropy energy	[J]
η	Viscosity	[Pa·s]
M _r	Residual magnetization	[A/m]
M _s	Saturation magnetization	[A/m]
λ	Wavelength	[m]

Constant	Definition	Value
μ_0	Permeability in vacuum	$4\pi \times 10^{-7} \text{ V}\cdot\text{s}/(\text{A}\cdot\text{m})$
k _B	Boltzmann constant	$1.380 \times 10^{-23} \text{ J/K}$
τ_0	Anisotropy energy	$(10^{-9}\text{-}10^{-10})$

Acknowledgements

Many individuals have assisted me during my graduate story, both at DISAT Department of Politecnico di Torino and at the Jozef Stefan Institute in Ljubljana where I could perform my thesis research.

I would like to begin by thanking my professor, Enrica Vernè, for all her guidance, and also Marta Miola for her assistance and advices. Special thank goes to Cristina Multari, for her patience and her precious help.

All the K7 staff of the Josef Stefan Institute of Ljubljana are gratefully acknowledged. In particular Nina Kostevšek deserve a great thank for the immense patience and the huge help that she gave me during the period I spent under her guidance.

I would like to thank my parents, my father Natalino and my mother Alessandra, my sisters Elena and Cinzia, with Mario and Lorenzo and Pito for their support and love. Also, all my family, Gino, Alo, Andre, Davide and my grandmother Meri are thanked.

All my friends, Reido, Pippo, Laur, Solda, Fez, Garde, Marti and Giulia are acknowledged for their constant support during my scholastic career.

References

- [1] N. Sanvicens and M. P. Marco, “Multifunctional nanoparticles – properties and prospects for their use in human medicine,” no. Figure 2, pp. 425–433, 2008.
- [2] L. Brannon-peppas and J. O. Blanchette, “Nanoparticle and targeted systems for cancer therapy ☆,” *Adv. Drug Deliv. Rev.*, vol. 64, pp. 206–212, 2012.
- [3] I. Brigger, C. Dubernet, and P. Couvreur, “Nanoparticles in cancer therapy and diagnosis ☆,” *Adv. Drug Deliv. Rev.*, vol. 64, pp. 24–36, 2012.
- [4] A. Kumar and M. Gupta, “Synthesis and surface engineering of iron oxide nanoparticles for biomedical applications,” vol. 26, pp. 3995–4021, 2005.
- [5] W. Wu, Z. Wu, T. Yu, and C. Jiang, “Recent progress on magnetic iron oxide nanoparticles : synthesis , surface functional strategies and biomedical applications,” vol. 023501.
- [6] P. Ñ. Tartaj, M. P. Ñ. Morales, and T. Gonza, “Advances in magnetic nanoparticles for biotechnology applications,” vol. 291, pp. 28–34, 2005.
- [7] S. Von Stillfried, R. Knüchel, F. Kiessling, and T. Lammers, “Iron oxide nanoparticles: Diagnostic, therapeutic and theranostic applications,” *Adv. Drug Deliv. Rev.*, p. #pagerange#, 2019.
- [8] M. K. Lima-tenório, E. A. Gómez, N. M. Ahmad, H. Fessi, and A. Elaissari, “Magnetic nanoparticles : In vivo cancer diagnosis and therapy,” *Int. J. Pharm.*, vol. 493, no. 1–2, pp. 313–327, 2015.
- [9] D. S. Mathew and R. Juang, “An overview of the structure and magnetism of spinel ferrite nanoparticles and their synthesis in microemulsions,” vol. 129, pp. 51–65, 2007.
- [10] Z. Hedayatnasab, F. Abnisa, W. Mohd, and A. Wan, “Review on magnetic nanoparticles for magnetic nano fl uid hyperthermia application,” *Mater. Des.*, vol. 123, pp. 174–196, 2017.
- [11] Z. Karimi, L. Karimi, and H. Shokrollahi, “Nano-magnetic particles used in biomedicine : Core and coating materials,” *Mater. Sci. Eng. C*, vol. 33, no. 5, pp. 2465–2475, 2013.
- [12] M. Faraji, Y. Yamini and M. Rezaee. Magnetic Nanoparticles: Synthesis, Stabilization, Functionalization, Characterization, and Applications. J. Iran. Chem. Soc., Vol. 7, No. 1, pp. 1-37 (2010).
- [13] S. Laurent, S. Dutz, U. O. Häfeli, and M. Mahmoudi, “Magnetic fl uid hyperthermia :

- Focus on superparamagnetic iron oxide nanoparticles,” *Adv. Colloid Interface Sci.*, vol. 166, no. 1–2, pp. 8–23, 2011.
- [14] R. V Mehta, “Synthesis of magnetic nanoparticles and their dispersions with special reference to applications in biomedicine and biotechnology,” *Mater. Sci. Eng. C*, vol. 79, pp. 901–916, 2017.
- [15] M. Hernández and C. Rinaldi, “Journal of Magnetism and Magnetic Materials Estimating the contribution of Brownian and Néel relaxation in a magnetic fluid through dynamic magnetic susceptibility,” *J. Magn. Magn. Mater.*, vol. 412, pp. 223–233, 2016.
- [16] A. Cristina and S. Samia, “crossmark,” *Prog. Nat. Sci. Mater. Int.*, vol. 26, no. 5, pp. 440–448, 2016.
- [17] P. Das, M. Colombo, and D. Prosperi, “Colloids and Surfaces B : Biointerfaces Recent advances in magnetic fluid hyperthermia for cancer therapy,” *Colloids Surfaces B Biointerfaces*, vol. 174, no. July 2018, pp. 42–55, 2019.
- [18] V. Patsula, M. Moskvina, S. Dutz, and D. Horák, “Journal of Physics and Chemistry of Solids Size-dependent magnetic properties of iron oxide nanoparticles,” *J. Phys. Chem. Solids*, vol. 88, pp. 24–30, 2016.
- [19] R. M. Fratila, “Introduction to Hyperthermia,” pp. 1–10, 2019.
- [20] Y. Choi, H. Lee, Y. Song, and D. Sohn, “Journal of Colloid and Interface Science Colloidal stability of iron oxide nanoparticles with multivalent polymer surfactants,” vol. 443, pp. 8–12, 2015.
- [21] D. Ramimoghadam, S. Bagheri, S. Bee, and A. Hamid, “Colloids and Surfaces B : Biointerfaces Stable monodisperse nanomagnetic colloidal suspensions : An overview,” *Colloids Surfaces B Biointerfaces*, vol. 133, pp. 388–411, 2015.
- [22] V. I. Shubayev, T. R. Pisanic, and S. Jin, “Magnetic nanoparticles for theragnostics ☆,” *Adv. Drug Deliv. Rev.*, vol. 61, no. 6, pp. 467–477, 2009.
- [23] M. Nedyalkova, B. Donkova, J. Romanova, G. Tzvetkov, S. Madurga, and V. Simeonov, “Iron oxide nanoparticles – In vivo / in vitro biomedical applications and in silico studies,” *Adv. Colloid Interface Sci.*, vol. 249, no. May, pp. 192–212, 2017.
- [24] L. Hajba and A. Guttman, “The use of magnetic nanoparticles in cancer theranostics : Toward handheld diagnostic devices,” *Biotechnol. Adv.*, vol. 34, no. 4, pp. 354–361, 2016.
- [25] Y. Yamini, “Arch Arch,” vol. 7, no. 1, pp. 1–37, 2010.

- [26] E. Cheraghipour, S. Javadpour, and A. R. Mehdizadeh, "Citrate capped superparamagnetic iron oxide nanoparticles used for hyperthermia therapy," vol. 2012, no. December, pp. 715–719, 2012.
- [27] J. Liu, C. Dai, and Y. Hu, "Aqueous aggregation behavior of citric acid coated magnetite nanoparticles : Effects of pH , cations , anions , and humic acid," *Environ. Res.*, vol. 161, no. July 2017, pp. 49–60, 2018.
- [28] L. Li, K. Y. Mak, C. W. Leung, K. Y. Chan, W. K. Chan, W. Zhong, and P. W. T. Pong, "Microelectronic Engineering Effect of synthesis conditions on the properties of citric-acid coated iron oxide nanoparticles," vol. 110, pp. 329–334, 2013.
- [29] A. I. N. Press, "Preparation and characterization of (3-aminopropyl) triethoxysilane-coated magnetite nanoparticles," vol. 279, pp. 210–217, 2004.
- [30] R. A. Bini, R. Fernando, C. Marques, F. J. Santos, J. A. Chaker, and M. Jafelicci, "Journal of Magnetism and Magnetic Materials Synthesis and functionalization of magnetite nanoparticles with different amino-functional alkoxysilanes," *J. Magn. Magn. Mater.*, vol. 324, no. 4, pp. 534–539, 2012.
- [31] D. Caruntu, B. L. Cushing, G. Caruntu, and C. J. O. Connor, "Attachment of Gold Nanograins onto Colloidal Magnetite Nanocrystals," no. 10, pp. 3398–3402, 2005.
- [32] A. N. Dizaji, M. Yilmaz, and E. Piskin, "Silver or gold deposition onto magnetite nanoparticles by using plant extracts as reducing and stabilizing agents," no. February, pp. 1–7, 2015.
- [33] V. Velasco, L. Muñoz, E. Mazario, and N. Menéndez, "Chemically synthesized Au – Fe₃O₄ nanostructures with controlled optical and magnetic properties," *J. Phys. D. Appl. Phys.*, vol. 035502, p. 35502.
- [34] K. C. F. Leung, S. Xuan, X. Zhu, D. Wang, C. P. Chak, and S. F. Lee et al. Gold and iron oxide hybrid nanocomposite materials. *Chemical Soc. Rev.* **41**, 1911–1928 (2012).
- [35] P. Albella, "Nanoscale Horizons bifunctional magnetic – plasmonic systems : three representative cases †," *Nanoscale Horizons*, vol. 2, pp. 205–216, 2017.
- [36] P. Malik and T. K. Mukherjee, "Recent advances in gold and silver nanoparticle based therapies for lung and breast cancers," *Int. J. Pharm.*, vol. 553, no. 1–2, pp. 483–509, 2018.
- [37] X. Zhang, Z. Liu, W. Shen, and S. Gurunathan, "Silver Nanoparticles : Synthesis , Characterization , Properties , Applications , and Therapeutic Approaches," 2016.
- [38] P. Zhao, N. Li, and D. Astruc, "State of the art in gold nanoparticle synthesis," vol.

- 257, no. July 2012, pp. 638–665, 2013.
- [39] X. Huang and M. A. El-sayed, “Gold nanoparticles : Optical properties and implementations in cancer diagnosis and photothermal therapy,” pp. 13–28, 2010.
 - [40] A. Moores, “The Plasmon Band in Noble Metal Nanoparticles : An Introduction to Theory and Applications The plasmon band in noble metal nanoparticles : an introduction to theory and applications,” no. May 2014, 2006.
 - [41] R. Article, “Gold nanoparticles as novel agents for cancer therapy,” vol. 85, no. February, pp. 101–113, 2012.
 - [42] Z. Li, M. Kawashita, N. Araki, M. Mitsumori, M. Hiraoka, and M. Doi, “Magnetite nanoparticles with high heating efficiencies for application in the hyperthermia of cancer,” *Mater. Sci. Eng. C*, vol. 30, no. 7, pp. 990–996, 2010.
 - [43] S. Campelj, D. Makovec, and M. Drofenik, “Preparation and properties of water-based,” no. May 2008, 2014.
 - [44] J. Daduang, A. Palasap, S. Daduang, P. Boonsiri, P. Suwannalert, and T. Limpai boon, “Gallic Acid Enhancement of Gold Nanoparticle Anticancer Activity in Cervical Cancer Cells,” vol. 16, pp. 169–174, 2015.
 - [45] Æ. N. Nin, “Synthesis and antibacterial activity of silver nanoparticles with different sizes,” pp. 1343–1348, 2008.
 - [46] T. Ahmad, “Reviewing the Tannic Acid Mediated Synthesis of Metal Nanoparticles,” vol. 2014, 2014.
 - [47] A. Saeed and U. Thahira, “Physica B : Condensed Matter Synthesis and characterization of stable silver nanoparticles , Ag-NPs : Discussion on the applications of Ag-NPs as antimicrobial agents,” *Phys. B Phys. Condens. Matter*, vol. 554, no. October 2018, pp. 21–30, 2019.
 - [48] E. Investigation, “Hybrid Self-Assembled Materials Constituted by Ferromagnetic Nanoparticles and Tannic Acid: a Theoretical and Experimental Investigation,” vol. 27, no. 4, pp. 727–734, 2016.